Chapter 4

MODELING AND SIMULATION

4.0 Introduction

A little work has been done on the mass transfer with chemical reaction in jet ejector. The principal focus of research in this chapter is to develop some significant experimental and modeling techniques for efficient design of multi nozzle jet ejectors. To achieve this goal the recent literature on mass transfer with and without chemical reaction along with experimental data developed for different gas liquid contactors are required to be adopted. An attempt is made for necessary modification and development to existing theories which can be used for our study.

On the basis of the variety of generated experimental data, multi nozzle-single nozzle, laboratory scale-industrial scale, horizontal installation-vertical installation etc., were utilized to develop general mathematical models. These developed models may be utilized to design multi nozzle jet ejector without experimental data on the basic available physicochemical properties like diffusivities, rate constant, equilibrium constant, Henerys' law constant etc.

In this chapter the mathematical model for absorption of chlorine in aqueous sodium hydroxide system were developed by making use of software like STATGRAPHICS and MATLAB. With the help of recent mathematical techniques the problem of gas-liquid mass transfer reduces to mathematical problem and solved by good mathematical models.

4.1 Prediction of absorption rate and reaction rate constant of chlorine into aqueous sodium hydroxide solution

The rate constant of chlorine absorption in aqueous $NaOH$ solution reported by different investigators has been summarized and presented in table 4.1.1 given below:

Table 4.1.1 : Rate constant for $Cl_2 - NaOH$ reaction as reported by different investigators

Author	Rate constant	Temperature
Morris (1946)	$5 \times 10^{14}\ m^3/kmol.s$	298K
Lifshitz and Perlmutter–Hayman (1961)	$(9 \pm 2) \times 10^{10}\ m^3/kmol.s$	283K
Lifshitz and Perlmutter–Hayman (1962)	Of the order of $10^{10}\ m^3/kmol.s$	283K
Spalding (1962)	Of the order of $10^{16} m^3/kmol.s$	298K
Sandall et al.(1981)	$2.7 \times 10^7\ m^3/kmol.s$	273K
Ashour et al. (1996)	$1.2 \times 10^9\ m^3/kmol.s$	298K

Ashour et al. (1996) studied the absorption of Cl_2 into aqueous bicarbonate and aqueous hydroxide solutions both experimentally and theoretically. They estimated the reaction rate coefficient of reaction between Cl_2 and OH^- over the temperature range of 293 – 312K:

$$k_{24} = 3.56 \times 10^{11} \exp\left(\frac{-1,617}{T}\right) \quad m^3/kmol.s \tag{4.1.1}$$

It is observed that there is disagreement in the literature about the value of the forward rate coefficient of absorption of Cl_2 into aqueous solution of $NaOH$.

In this section, correlation to estimate the rate constant k for absorption of Cl_2 in to aqueous solution of sodium hydroxide in jet ejector is developed using penetration model. The results obtained by this model are compared with the experimental values. Apart from this a mathematical model is also developed to estimate rate of absorption (R_A) and enhancement factor (β) which may be utilized to estimate further interfacial area a in the section 4.4.

4.1.1 Model for the absorption of chlorine into aqueous $NaOH$ solution based on penetration theory

When Cl_2 is absorbed in aqueous $NaOH$ solution, the following reactions may take place:

$$Cl_2 + H_2O \overset{K_1,k_1}{\longleftrightarrow} HOCl + H^+ + Cl^- \tag{4.1.2}$$

$$Cl_2 + OH^- \overset{K_2,k_2}{\longleftrightarrow} HOCl + Cl^- \tag{4.1.3}$$

$$HOCl + OH^- \overset{K_3,k_3}{\longleftrightarrow} OCl^- + H_2O \tag{4.1.4}$$

$$H_2O \overset{K_4,k_4}{\longleftrightarrow} OH^- + H^+ \tag{4.1.5}$$

In this model, all reactions are assumed to be reversible. However reaction (4.1.2) and (4.1.3) have finite reaction rates, whereas reaction (4.1.4) and (4.1.5) are assumed to be instantaneous.

Here three equilibrium constants K_1, K_3 and K_4 are independent and remaining K_2 can be obtained by following equation:

$$K_2 = \frac{K_1}{K_4}$$

The concentrations of chemical species that are present in aqueous $NaOH$ solutions are renamed as follows:

$$w_1 = C_{Cl_2}$$

$$w_2 = C_{HOCl}$$

$$w_3 = C_{Cl^-}$$

$$w_4 = C_{H^+}$$

$$w_5 = C_{OCl^-}$$

$$w_6 = C_{OH^-}$$

$$w_7 = C_{H_2O}$$

$$w_8 = C_{Na^+} = C_{NaOH,initial}$$

4.1.1.1 Concentration of an individual chemical species in bulk of liquid

Assuming all the reactions are at equilibrium the following equations can be derived by overall mass balance.

Chlorine balance:

$$2w_1^0 + w_2^0 + w_3^0 + w_5^0 = LC_{NaOH,initial} \tag{4.1.6}$$

where L is the molar ratio of chlorine to $NaOH$ initially.

Hydrogen balance:

$$w_2^0 + w_4^0 + w_6^0 + 2w_7^0 = C_{NaOH,initial} + 2C_{H_2O,initial} \tag{4.1.7}$$

Oxygen balance:

$$w_2^0 + w_5^0 + w_6^0 + w_7^0 = C_{H_2O,initial} + C_{NaOH,initial} \tag{4.1.8}$$

Electroneutrality Balance:

$$w_4^0 + w_8^0 - w_3^0 - w_5^0 - w_6^0 = 0 \tag{4.1.9}$$

$$w_8^0 = C_{Na^+} = C_{NaOH,initial} \tag{4.1.10}$$

As the reactions are at equilibrium the independent equilibrium constants are:

$$K_1 = \frac{w_2^0 w_3^0 w_4^0}{w_1^0} \tag{4.1.11}$$

$$K_2 = \frac{w_2^0 w_3^0}{w_1^0 w_6^0} \tag{4.1.12}$$

$$K_3 = \frac{w_5^0}{w_2^0 w_6^0} \tag{4.1.13}$$

$$K_4 = w_6^0 w_4^0 \tag{4.1.14}$$

We have 7 unknowns and 7 algebraic independent equations.

These equations are linear system of equations and may be solved by minimal residual technique using MATLAB to get w_1^0 *to* w_7^0 (which converge to the solution).

It may be noted that in case of aqueous $NaOH$ solution do not contain any chlorine initially (means L=0) then

$$w_1^0 = w_2^0 = w_3^0 = w_5^0 = 0 \tag{4.1.15}$$

$$w_6^0 = C_{NaOH,initial} \tag{4.1.16}$$

4.1.1.2 Mass balance at interface applying Higbie's penetration model

In jet ejector liquid jet ensuing at high velocity from nozzles situated at top, pulls the gaseous phase in to the jet. The gaseous stream is broken into small bubbles due to high kinetic energy of liquid jet and the gas-liquid comes in contact for a short time at about 1/10 second. The mass transfer takes place from the interface of bubble to the encircled liquid. To adopt penetration model let, 'x', be the distance from the interface of the bubble. So x = 0 denotes the gas-liquid interface. The liquid coming out of jet travel as free jet from outlet of multi nozzle to entry of throat where the surrounding gas gets entrained in it through its exposed outer surface. This liquid stream with bubbles then travels in uniform cross section of throat and at the end it passes through a conical diffuser section. Let Z be the length along the axis of liquid jet Z = 0 at the out let of nozzles and $Z = Z_{tot}$ at the outlet of the jet ejector. Let t, be the time of exposure and may be computed by

$$t = \frac{commulative\ volume\ till\ the\ posstion,\ Z}{total\ volumetric\ flow\ rate}$$

To compute volume between outlets of nozzles to inlet of throat, it is assumed that fluid travels through cylindrical passage having diameter equal to inside diameter of nozzle and length L_{TN}.

By assuming all reactions reversible, the following reaction rate expression may be written.

$$r_1 = -k_1 w_1 + \frac{k_1}{K_1} w_2 w_3 w_4 \tag{4.1.17}$$

$$r_2 = -k_2 w_1 w_6 + \frac{k_2}{K_2} w_2 w_3 \tag{4.1.18}$$

The reactions (4.1.4) and (4.1.5) are instantaneous having large values of rate of reaction therefore are eliminated. We also assume that:

- Reactions are at equilibrium.
- The diffusivity of ionic spices are equal.
- The fluxes of the nonvolatile species at interface are equal to zero.

By considering the mass balance following differential equation are derived:

Cl_2 balance

$$\frac{\partial w_1}{\partial t} = D_1 \frac{\partial^2 w_1}{\partial x^2} + r_1 + r_2 \tag{4.1.19}$$

Cl_2 / Cl^- balance

$$\frac{\partial w_1}{\partial t} + \frac{\partial w_3}{\partial t} = D_1 \frac{\partial^2 w_1}{\partial x^2} + D_3 \frac{\partial^2 w_3}{\partial x^2} \tag{4.1.20}$$

Total chlorine balance

$$2\frac{\partial w_1}{\partial t} + \frac{\partial w_2}{\partial t} + \frac{\partial w_3}{\partial t} + \frac{\partial w_5}{\partial t} = 2D_1 \frac{\partial^2 w_1}{\partial x^2} + D_2 \frac{\partial^2 w_2}{\partial x^2} + D_3 \frac{\partial^2 w_3}{\partial x^2} + D_4 \frac{\partial^2 w_5}{\partial x^2} \tag{4.1.21}$$

Electroneutrality Balance:

$$w_4 + w_8 - w_3 - w_5 - w_6 = 0 \tag{4.1.22}$$

Where $w_8 = C_{Na^+} = C_{NaOH,initial}$

As it is assumed all reactions are reversible hence the instantaneous reactions are also at equilibrium and their equilibrium constant may be written as follow:

$$K_3 = \frac{w_5}{w_2 w_6} \tag{4.1.23}$$

$$K_4 = w_4 w_6 \tag{4.1.24}$$

There are 6 unknowns and 6 partial differential equations/algebraic equations which can be solved for the concentrations of all chemical species.

Initial condition and boundary conditions

At $t = 0$ (for all $x \geq 0$) and at $x = \infty$ (for all $t \geq 0$)

the concentration of chemical species are equal to bulk concentrations in liquid.

$$w_i = w_i^0, i = 1 \; to \; 6 \tag{4.1.25}$$

$i.e. (w_1 = w_1^0,\ w_2 = w_2^0,\ w_3 = w_3^0,\ w_4 = w_4^0,\ w_5 = w_5^0,\ w_6 = w_6^0)$

Boundary conditions at interface

At the interface of gas-liquid $x = 0$

For non volatile species

$$\frac{\partial w_j}{\partial x} = 0, at\ x = 0, t > 0 \tag{4.1.26}$$

for all j except j =1 (Cl_2)

For volatile species (Cl_2), the rate of absorption per unit interfacial area may be written as

$$-D_j \frac{\partial w_j}{\partial x} = k_{g,j}[p_j - H_{ej}\, w_j\,(0,t)] \tag{4.1.27}$$

Here in our system there is only one volatile species i.e. chlorine and hence $j = 1$. So we may write $D_1 = D_j$, $w_1 = w_j$ and $H_{ej} = H_{e1}$

The equation (4.1.27) may be re-written as

$$-D_1 \frac{\partial w_1}{\partial x} = k_{g,1}[p_1 - H_{e1}\, w_1\,(0,t)] \tag{4.1.28}$$

The value of the true gas side mass transfer coefficient, $k_{g,1,}$ for chlorine required in equation (4.1.27) was predicted from the correlation reported by Lydersen (1983, pp. 129) which is about 0.000432.

Where H_{e1} is the physical equilibrium constant (Henry's law constant) of Cl_2.

For chlorine-aqueous $NaOH$ solution the equation (4.1.28) may be re-written as

$$p_1 + \left(\frac{D_1}{k_{g,1}}\right)\frac{\partial w_1}{\partial x} = H_{e1}\, w_1\,(0,t)$$

Now $D_1 \cong 1.68 \times 10^{-9}$ $(table\ A3.4)$ and $k_{g,1} \cong 3.7 \times 10^{-4}$ $(table\ A4.1)$

Therefore $D_1/k_{g,1}$ is negligible.

Hence,

$$p_1^* = [H_{e1}\, w_1\,(0,t)]$$

The boundary condition for pure Cl_2 at the gas liquid inference reduces to

$$w_1(0,t) = w_1^* = \frac{p_1}{H_{e1}}\ at\ x = 0 \quad t > 0 \tag{4.1.29}$$

4.1.1.3 Numerical solution and its implementation

Equation (4.1.19) - (4.1.29) represents a mathematical model to obtain the values of $w_1, w_2, \ldots\ldots\ldots w_7$. It is not possible to obtain analytical solution and therefore we have used Finite Difference Method (FDM) to transform each partial differential equation of the model into the system of ordinary differential equations in t.

We choose following finite difference expressions to approximate the partial derivatives:

$$\frac{\partial w_{i,j}}{\partial x} = \frac{1}{2h_j}\left[w_{i,j+1} - w_{i,j-1}\right] + higher\ order\ terms \tag{4.1.30}$$

$$\frac{\partial w_{i,j}}{\partial x^2} = \frac{1}{h_j^2}\left[-2w_{i,j} + w_{i,j+1} + w_{i,j-1}\right] + \ higher\ order\ terms \tag{4.1.31}$$

where i refer to the i^{th} chemical species, j, refers to the spatial node number and $h_j = x_{j+1} - x_j$. Typical values for the initial nodal spacing h_0 at the gas-liquid interface are about 10^{-4}. The transformed system of ordinary differential equation in t can be solved by MATLAB software by using ODE15 solver with preconditioning technique and with special Jacobi pre-conditioner.

This simulation gives w_1 and $\left(\frac{\partial w_1}{\partial x}\right)$ simultaneously and which gives the average rate of absorption of Cl_2 per unit interfacial area (flux). This may be written as

$$N_{Cl_2} = \frac{D_1}{t_e}\int_0^{t_e}\left(\frac{\partial w_1}{\partial x}\right)(0,t)dt \tag{4.1.32}$$

The gas liquid exposure time for the jet ejector may be stated as

$$t_e = \frac{Total\ volume\ of\ Jet\ ejector}{Sum\ of\ volumetric\ flow\ rate\ of\ aqueous\ solution\ and\ gas} \tag{4.1.33}$$

$$t_e = \frac{V_J}{F_L + F_G}$$

Similarly, the enhancement factor of Cl_2 may be determined from the following equation

$$\beta = \frac{N_{Cl_2}}{k_L^0(w_1^* - w_1^0)} \tag{4.1.34}$$

where w_1^* *and* w_1^0 are interfacial and bulk concentrations of Cl_2 in the liquid respectively and k_L^0 is the liquid phase mass transfer coefficient for physical absorption of Cl_2 and is given by

$$k_L^0 = 2\sqrt{\frac{D_1}{\pi t_e}} \tag{4.1.35}$$

To solve the mathematical model the diffusivities of different species and Henry's law constant of Cl_2 are required which are tabulated in Table (4.1.2). We also need the equilibrium constants and the forward rate coefficients of all chemical reactions (4.1.2) through (4.1.5), which are tabulated in Table (4.1.3).

Table 4.1.2: Henery's law constant of Cl_2 and diffusion coefficients of Cl_2 (D_1), $HOCl$ (D_2), and OH^- (D_6) (Ashour et al., 1996)

T K	$[NaOH]_{initial}$ $kmol/m^3$	H_1 $atm.m^3/kmol$	$10^9 D_1$ m^2/s	$10^9 D_2$ m^2/s	$10^9 D_6$ m^2/s
293	0.09985	13.44	1.29	1.34	2.99
298	0.10000	16.36	1.47	1.54	3.43
303	0.09960	19.55	1.68	1.75	3.89
312	0.09970	26.98	2.05	2.14	4.76

Table 4.1.3: Values for Equilibrium constants of Reactions (4.1.2) and (4.1.5) at various temperatures, (Ashour et al., 1996)

T K	$10^4 K_1$ $(kmo/m^3)^2$	$10^{-10} K_2$	$10^{-6} K_3$ $m^3/kmol$	$10^{14} K_4$ $10^{14} K_4 (kmo/m^3)^2$	k_1 $m^3/kmol\ s$
293	3.890	5.722	3.726	0.6798	1.157
298	4.500	4.491	2.790	1.002	16.4
303	5.181	3.580	2.109	1.447	23
308	5.938	2.895	1.609	2.051	32
313	6.776	2.371	1.238	2.858	44

* rate of reactions r_3 and r_4 are instantaneous having large value of k and are eliminated.

4.1.2 Results and discussion

The penetration model has been used to develop mathematical model for absorption of Cl_2 in to aqueous solution of sodium hydroxide. The mathematical model to predict absorpaiton rate is presented by equation (4.1.19) - (4.1.29).

To solve this model the value of k_1, k_2, k_3 and k_4 were required. The value of k_1 was determined by the correlation given by Brian et al. (1966)

$$k_1 = 1.4527 \times 10^{10}\, exp.\left(\frac{-6138.6}{T}\right) \qquad (4.1.36)$$

The reaction R_3 and R_4 are instantaneous hence eliminated.

There is large variation in the value of k_2 in the literature as clear from Table (4.1.1). Hence attempt has been made to estimate value of k_2 by using data obtained for absorption of Cl_2 in aqueous sodium hydroxide solution in the jet ejector. The value of k_2 was adjusted until the theoretically predicted rate of absorption was within 1% of the experimentally measured rate of absorption of Cl_2.

Thus following correlation is developed to predict the value of k_2 :

$$k_2 = 3.39 \times 10^{11}\, exp.\left(-\frac{1610}{T}\right) \qquad (4.1.37)$$

The predicted values of k_{24} from equation (4.1.1) reported by Ashour et al. (1996) and predicted value of k_2 from equation (4.1.37) by proposed model, along with the value obtained from the experimental result of present work are presented in table (4.1.4) and plotted in figure (4.1.1) and (4.1.1b).

Table 4.1.4 : The values of rate constants for reaction 4.1.3, k_2, at atmospheric pressure for Cl_2-Aqueous $NaOH$ system

T K	$[NaOH]_{initial}$ $kmol/m^3$	$10^6 L$ m^3/s	$10^4 t_e$ $sec.$	$10^4 k_{L,1}^0$ m/s	Measured $10^4 R_A$ $\frac{kmol}{m^2.s}$ Ashour et al. (1996)	Measured $10^4 R_A$ $\frac{kmol}{m^2.s}$ Present work	Estimated $10^9 k_2$ $\frac{m^3}{kmol.s}$ present model)	Predicted $10^9 k_2$ $\frac{m^3}{kmol.s}$ Ashour et al. (1996) Eq.(4.1.1)	Predicted $10^9 k_2$ $\frac{m^3}{kmol.s}$ present model Eq.(4.1.37)
293	0.09985	0.787	7.19	4.7805	7.94	-	-	1.42	1.39
298	0.10000	0.836	6.89	5.2136	7.73	-	-	1.57	1.5
303	0.09960	0.750	7.63	5.2945	7.60	-	-	1.7	1.7
312	0.09970	0.829	6.86	6.1669	7.98	-	-	2	1.95
303	0.03	110	69.9	0.0986	-	0.05	1.669	-	-

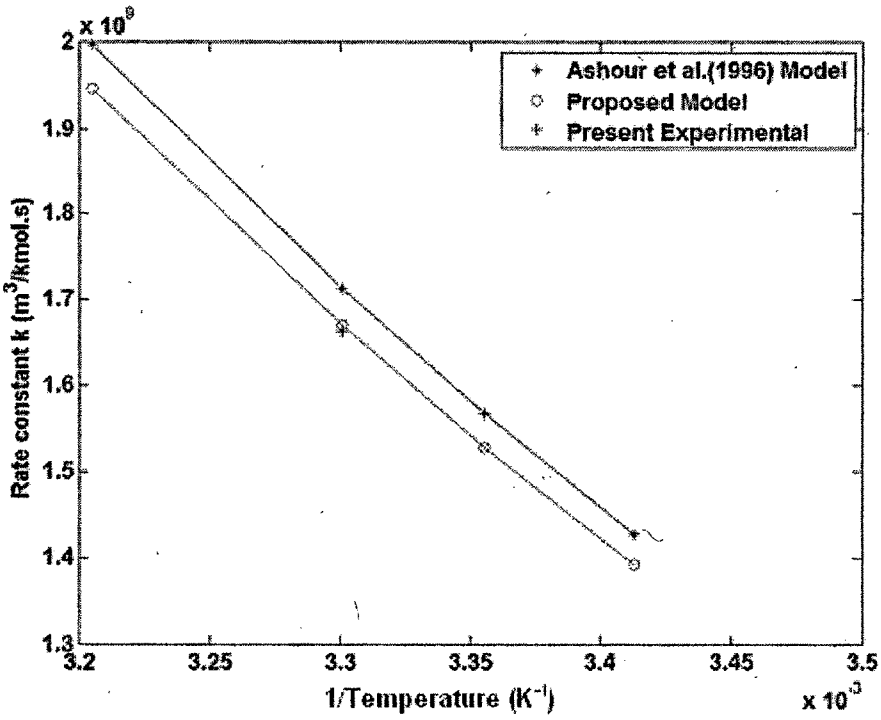

Figure 4.1.1 : Comparison of *k* obtained by Ashour et al. (1996), proposed mathematical model and experimental result by Ashour et al. (1996) with present experimental result over the temperature range of 293-312 K

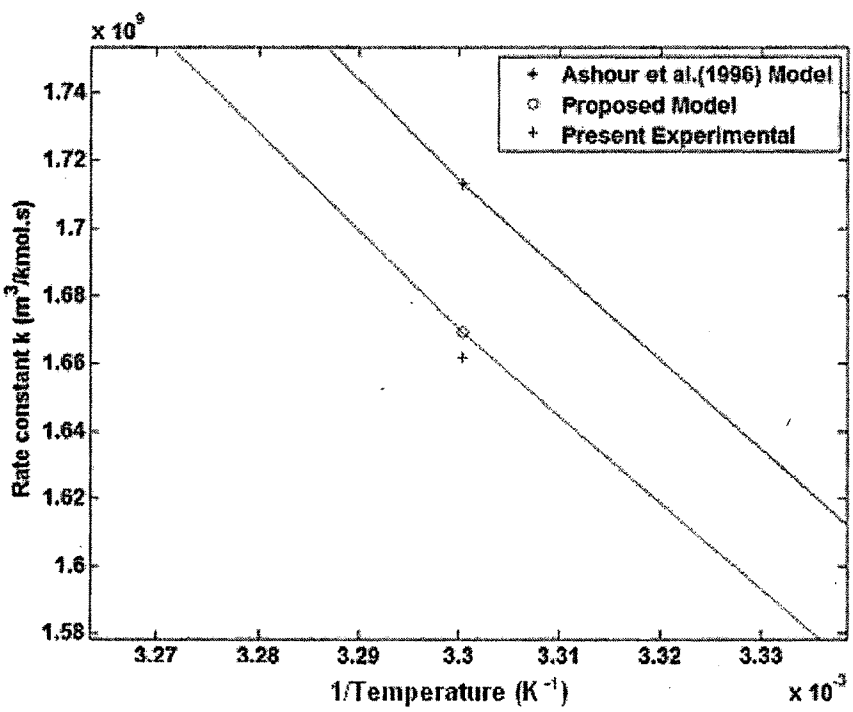

Figure 4.1.1a : Detailed view of figure (4.1.1) at a temperature T^{-1} =3.3x10^{-3}

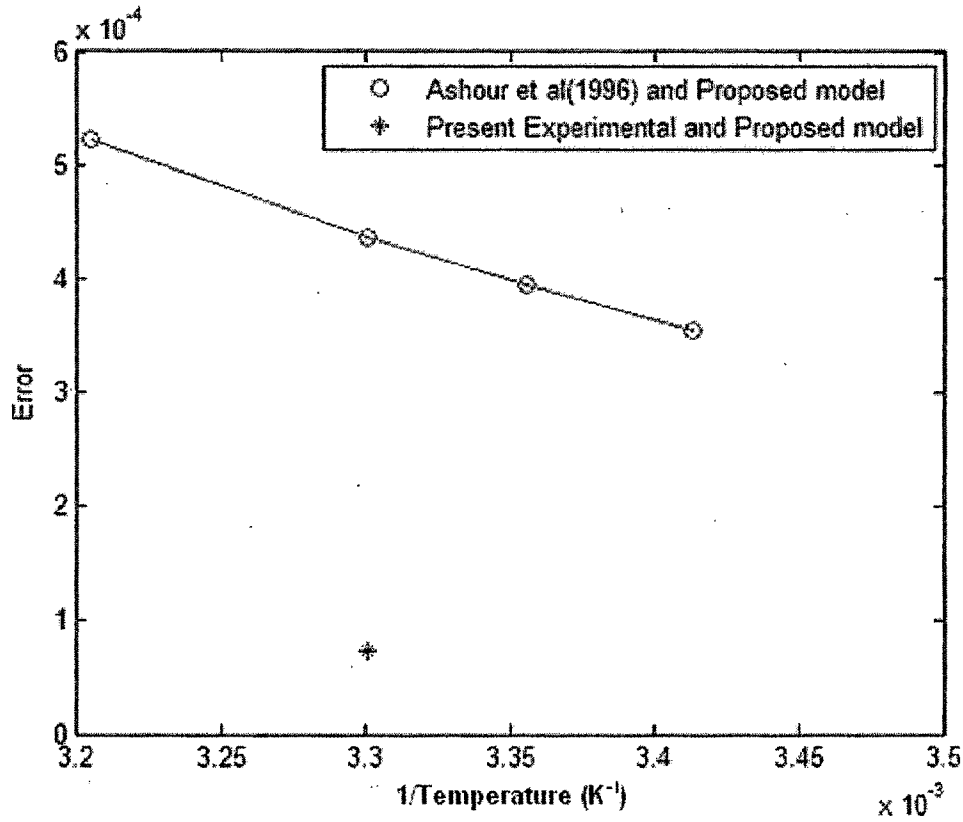

Figure 4.1.2 : Error estimates for k_2 and Ashour et al. (1996)

The experimental value and value predicted by present model (equation 4.1.37) are comparable. The values estimated by Ashour et al. (1996) are a little higher for which error is estimated. The error in-general may be defined as the absolute value of difference between estimated or measured value and actual value. Here error is defined as follow:

$$Error = |k \text{ predicted by Ashour (1996) model} - k \text{ predicted by proposed model}|$$

The error estimates for Ashour et al. (1996) and proposed model along with error between proposed model and present experimental value are presented in figure (4.1.2). The error between proposed model and Ashour et al. (1996) are less than 5.2 x 10^{-4} and the error between proposed model and experimental value is about 0.8 x 10^{-4}. As the error is very less it may be concluded that the proposed model is good.

The figure (4.1.3) presents R_A vs $C_{Ag,in,}$ (C_{B0} as parameter). The values obtained by experiment and by proposed model are in good agreement.Thus the chemical absorption mechanism proposed in the present work may be considered to be correct.

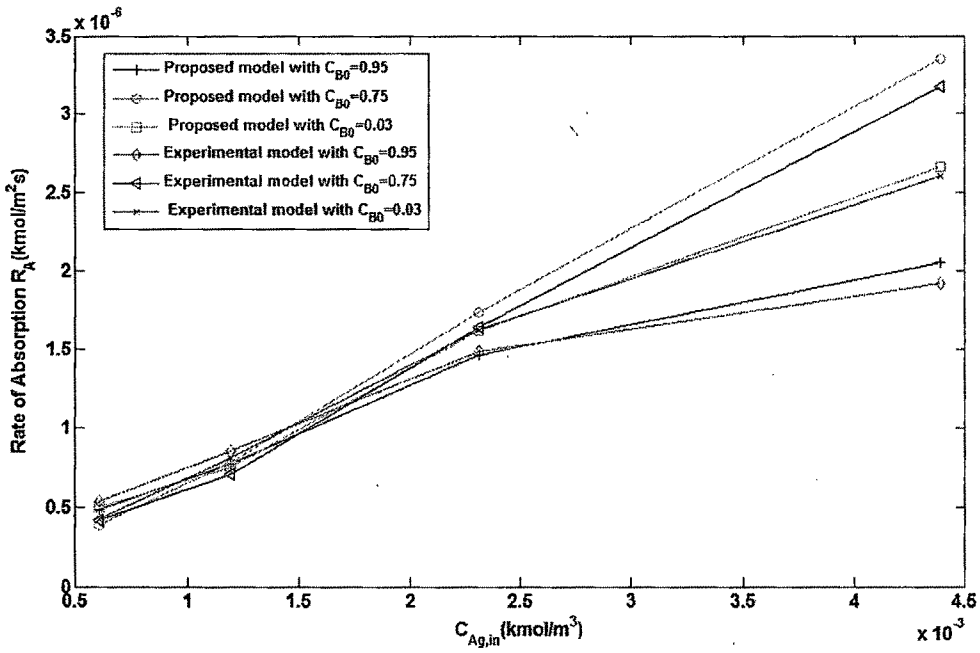

Figure 4.1.3 : Comparison between the values for rate of absorption obtained experimentally and predicted by proposed model with respect to C_{A0} at different C_{B0}

4.1.3 Conclusion

- The value R_A obtained by experiment and predicted from the proposed model are in good agreement. Hence, the proposed mathematical model may be used to predict the value of reaction rate, R_A. These values may be further utilized to predict enhancement factor β and interfacial area using following co-relations:

$$\beta = \frac{R_A}{k_L^0(C_A^* - C_A^0)}$$

$$a = \frac{R_a . a}{R_a}$$

- The correlation obtained to estimate rate constant for forward part of absorption of chlorine in aqueous $NaOH$ is

$$k_2 = 3.39 \times 10^{11}\, exp.\left(-\frac{1610}{T}\right)$$

4.2 Effect of the diffusivities on absorption of chlorine into aqueous sodium hydroxide solution

The absorption of chlorine into aqueous sodium hydroxide solutions is one of the important systems having industrial importance and also is of theoretical interest.

Danckwerts (1950a and 1950b) and Sherwood and Pigford (1952) showed that absorption rate could be predicted by the penetration theory for absorption accompanied by an instantaneous irreversible reaction of the type $A + B \rightarrow E$.

Spalding (1962) studied the absorption rate of Cl_2 into water and aqueous solutions of H_2SO_4 and $NaOH$ using liquid-jet column. They have also established that the absorption rate of Cl_2 will be affected by the reactions (4.2.1) and /or (4.2.2):

$$Cl_2 + H_2O \rightleftharpoons HOCl + H^+ + Cl^- \qquad (4.2.1)$$

or

$$Cl_2 + OH^- \rightleftharpoons HOCl + Cl^- \qquad (4.2.2)$$

depending upon the pH value of the solution.

Further, they have observed that when pH value was higher than 12.6 (i.e. OH^- concentration more than 0.04 $gmol/l$ the forward part of reaction (4.2.2) was rate-controlling and the effect of this reaction on the absorption rate could be predicted by the penetration theory for absorption accompanied by an instantaneous irreversible reaction.

Brian et al. (1965) studied gas absorption accompanied by a two-step chemical reaction, $A + B \rightarrow C$ followed by $C + B \rightarrow E$. They have considered both steps irreversible and of finite reaction rates and presented the theoretical analysis based on both, the film theory and the penetration theory, with numerical solutions for the enhancement factor, β.

Takahashi et al. (1967) used two different types of absorbers viz. liquid-jet column and a stop-cock type absorber to study the absorption rates of Cl_2 into aqueous $NaOH$ (0.05 to 0.2 $gmol/l$). The predicated absorption rate using penetration theory was in good agreement with experimental results.

Hikita et al. (1972) studied gas absorption of two-step chemical reaction, $A + B \overset{K_1}{\leftrightarrow} C$ followed by $C + B \overset{K_2}{\leftrightarrow} E$, accompanied by $A + E \rightleftharpoons 2C$. They have studied the effect of ratio of chemical equilibrium constants, P (which is defined as K_1/K_2), on enhancement factor, β. They have developed mathematical models for $P = 0$, finite value and ∞, for equal diffusivity and unequal diffusivities of species on the basis of penetration theory.

Hikita et al. (1973) stated that in case of strong hydroxide solution the forward part of reaction (4.2.2) is not only reaction which governs the absorption rate of Cl_2 but the rapid reaction

$$HOCl + OH^- \rightleftharpoons OCl^- + H_2O \qquad (4.2.3)$$

also affects the absorption rate of Cl_2 as the equilibrium constant of this reaction is very large.

In this section, the author has developed a mathematical model to study the effect of diffusivities on the enhancement factor and analyzed the experimental data obtained by him and Hikita et al. (1973) on the basis of the penetration theory for gas absorption accompanied by a two step instantaneous chemical reaction. In this work, the rate of absorption in the jet ejector is studied by using Cl_2 - aqueous $NaOH$ system at 30^0C.

4.2.1 Mechanism of chemical absorption

Spalding (1962) mentioned that, when OH^- concentration is more than $0.04\ g\ mol/l$ the forward part of reaction (4.2.2) is rate-controlling which affects the absorption rate.

Hikita et al. (1973) stated that $HOCl$ (hypochlorous acid) formed by reaction (4.2.2) can react again with OH^- ions results in rapid reaction (4.2.3) having equilibrium constant $K = 2.2 \times 10^6\ l/gmole$. Hence considering two step mechanism of the reaction (absorption) between Cl_2 and an aqueous hydroxide solution, may be written as follows:

$$Cl_2 + OH^- \overset{\leftarrow r_2, r_1 \rightarrow}{\longleftrightarrow} HOCl + Cl^- \qquad (4.2.4)$$

$$HOCl + OH^- \overset{\leftarrow r_4, r_3 \rightarrow}{\longleftrightarrow} OCl^- + H_2O \qquad (4.2.5)$$

$$Cl_2 + 2OH^- \longleftrightarrow CL^- + OCl^- + H_2O \qquad (4.2.6)$$

The values of the equilibrium constants of reactions (4.2.2) and (4.2.3) are K_1 and K_2. They are stated as follows:

$$K_1 = \frac{[HOCl][Cl^-]}{[Cl_2][OH^-]}$$

$$K_2 = \frac{[OCl^-]}{[HOCl][OH^-]}$$

The values of K_1 and K_2 at 30^0C is given by 3.1×10^{10} (Connick et al., 1959) and $2.2 \times 10^6\ l/gmole$ (Morris, 1966) respectively.

The hydrolysis of dissolved Cl_2 with water takes place according to the reaction

$$Cl_2 + H_2O \rightleftarrows HOCl + H^+ + Cl^- \qquad (4.2.1)$$

The equilibrium constant of this reaction is given by

$$K_3 = \frac{[HOCL][H^+][Cl^-]}{[Cl_2]}$$

and having value $4.5 \times 10^{-4}(gmole/l)^2$ (Connick et al.,1959) at 30^0C.

The values of K_3 is very low compared to the value of K_1, and hence reaction (4.2.1) will not have a significant contribution to the total reaction rate of Cl_2

Therefore, the absorption of Cl_2 into aqueous hydroxide solutions can be considered as an instantaneous two-step reaction, which is equivalent to say that reaction (4.2.4) followed by reaction (4.2.5) and having over all reaction (4.2.6).

4.2.2 Mathematical models related to absorption

Enhancement factor, β

The rate of absorption of reactant A (gas) with instantaneous chemical reaction can be predicted by summing

(a) Amount of A diffuse away unreacted and

(b) Amount of reacted A (in the form of C) diffuse away from the gas-liquid interface.

Therefore,

$$-N_{A_i} = D_A\left(\frac{\partial A}{\partial x}\right)_{x=0} + \frac{1}{2}D_C\left(\frac{\partial C}{\partial x}\right)_{x=0} \tag{4.2.7}$$

The integration of equation (4.2.7) from time zero to the total exposure time t_e gives the average absorption rate and which may be written as:

$$N_A = \frac{1}{t_e}\int_0^{t_e} N_{A_i}\,dt$$

$$= \frac{1}{t_e}\int_0^{t_e}\left[-D_A\left(\frac{\partial A}{\partial x}\right)_{x=0} - \frac{1}{2}D_C\left(\frac{\partial C}{\partial x}\right)_{x=0}\right]dt \tag{4.2.8}$$

The average absorption rate of A in absence of the chemical reaction is given by the well-known Higbie equation

$$N_A^* = 2C_{Ai}^*\sqrt{\frac{D_A}{\pi t}} \tag{4.2.9}$$

It is known that the enhancement factor is the ratio of average rates of absorption with chemical reaction and without chemical reaction. Therefore from equation (4.2.8) and (4.2.9):

$$\beta = \frac{N_A}{N_A^*} = -\frac{1}{2C_{Ai}^*}\sqrt{\frac{\pi D_A}{t_e}}\int_0^{t_e}\left[\left(\frac{\partial A}{\partial x}\right)_{x=0} + \left(\frac{D_C}{D_A}\right)\left(\frac{\partial C}{\partial x}\right)_{x=0}\right] \tag{4.2.10}$$

Desorption of the $HOCl$

Lahiri et al. (1983) studied the process of desorption of the intermediate product hypochlorous acid, $HClO$, during the process of absorption of Cl_2 in aqueous alkaline hydroxides. They gave correlation for the rate of desorption of the $HOCl$ product:

$$R_{d,HOCl} = \sqrt{\left(\frac{D_C}{\pi t}\right)}\left\{\frac{C_{HOCl,\ x_1} - C_{HOCl,\ x=0}}{\operatorname{erf}\left[\sqrt{\left(\frac{D_A}{D_C}\right)}\sigma_1\right]}\right\} \tag{4.2.10a}$$

Therefore, average rate of desorption over a total exposure time, t_e, is given by

$$\bar{R}_{d,HOCl} = \frac{1}{t_e}\int_0^{t_e} R_{d,HOCl}\,dt$$

$$= 2\sqrt{\frac{D_C}{\pi t_e}}\left\{\frac{C_{HOCl,\ x_1} - C_{HOCl,\ x=0}}{\text{erf}\left[\sqrt{\left(\frac{D_A}{D_C}\right)}\sigma_1\right]}\right\}$$

$$= \frac{1}{\text{erf}\left[\sqrt{\frac{D_A}{D_C}}\sigma_1\right]} 2\sqrt{\frac{D_A}{\pi t_e}}\sqrt{\frac{D_C}{D_A}}\left(C_{HOCl,\ x_1} - C_{HOCl,\ x=0}\right) \qquad (4.2.10b)$$

Substituting,

$\emptyset_{d,HOCl}$ = enhancement factor for desorption

$$= \frac{1}{\text{erf}\left[\sqrt{\frac{D_A}{D_C}}\sigma_1\right]}$$

and

k_L = true liquid side mass transfer coefficient without chemical reaction.

$$= 2\sqrt{\frac{D_A}{\pi t_e}}$$

The equation (4.2.10b) will become:

$$\bar{R}_{d,HOCl} = \emptyset_{d,HOCl} \cdot k_L \cdot \sqrt{\left(\frac{D_C}{D_A}\right)}\left(C_{HOCl,\ x_1} - C_{HOCl,\ x=0}\right) \qquad (4.2.10c)$$

One reaction-plane model

Hikita et al. (1972) developed the model based on penetration theory for absorption with instantaneous chemical reaction and found that for $P = 0$ there exists only one reaction plane, where the over-all reaction of reactions $A + B \rightleftharpoons C$ and $C + B \rightleftharpoons E$ is $A + 2B \rightleftharpoons E$, proceeds irreversibly. The average rate of absorption of the solute gas can be calculated by following equations which were derived by Danckwerts (1950) and Sherwood and Pigford (1952).

$$N_A = \beta\left(2C_{Ai}^{*}\sqrt{\frac{D_A}{\pi t_e}}\right) \qquad (4.2.11)$$

$$\beta = \frac{1}{\text{erf}(\sigma)} \tag{4.2.12}$$

Where σ is root of the equation

$$erfc\left(\sqrt{\frac{D_A}{D_B}}\sigma\right)\exp\left[\left(\frac{D_A}{D_B}-1\right)\sigma^2\right] = \sqrt{\frac{D_B}{D_A}}\,\frac{C_{B0}}{2C_{Ai}^*}\text{erf}(\sigma) \tag{4.2.13}$$

This absorption mechanism is called a "one reaction-plane model".

Two reaction plane model

Hikita et al. (1972) developed a two reaction plane model when $P = \infty$ and established the fact that two reaction planes are formed within the liquid, which are as follows:

- The reaction $A + E \rightleftharpoons 2C$ which is the sum of forward part of the first-step reaction $(A + B \rightleftharpoons C)$ and the backward part of second step reaction $(C + B \rightleftharpoons E)$ take place irreversibly at the first reaction plane (which is located closer to the gas-liquid interface)
- The reaction $(C + B \rightleftharpoons E)$ take place irreversibly at the second reaction plane.

Further, the absorption rate may be calculated by equation (4.2.11) and following equation:

$$\beta = \frac{1}{\text{erf}(\sigma_1)} \tag{4.2.14}$$

where σ_1 is the root of following equations.

$$2erfc\left(\sqrt{\frac{D_A}{D_B}}\sigma_2\right)\exp\left[\left(\frac{D_A}{D_C}-1\right)\sigma_1^2+\left(\frac{D_A}{D_B}-\frac{D_A}{D_C}\right)\sigma_2^2\right] = \sqrt{\frac{D_B}{D_A}}\,\frac{C_{B0}}{C_{Ai}^*}\text{erf}(\sigma_1) \tag{4.2.15}$$

$$erfc\left(\sqrt{\frac{D_A}{D_E}}\sigma_1\right)\exp\left[\left(\frac{D_A}{D_E}-1\right)\sigma_1^2\right] - 2erfc\left(\sqrt{\frac{D_A}{D_E}}\,\sigma_2\right)$$

$$\exp\left[\left(\frac{D_A}{D_C}-1\right)\sigma_1^2+\left(\frac{D_A}{D_E}-\frac{D_A}{D_C}\right)\sigma_2^2\right] = \sqrt{\frac{D_E}{D_A}}\,\frac{C_{E0}}{C_{Ai}^*}\text{erf}(\sigma_1) \tag{4.2.16}$$

Two reaction plane model for absorption of Cl_2 into aqueous $NaOH$ solution

The reaction scheme for the $Cl_2 - aqueous\ NaOH$ system studied in this work is similar to the work of Hikita et al. (1972). The present reaction system (Equation (4.2.4) and (4.2.5)) may be described in the form

$$A + B \rightleftharpoons C + C$$

and

$$C + B \rightleftharpoons E$$

The present system is different than the work of Hikita et al. (1972) due to presence of C' which was not present in Hikita et al. (1972). However the species $C'(NaCl)$ is non-reactive. Hence it does not affect reactive mechanism.

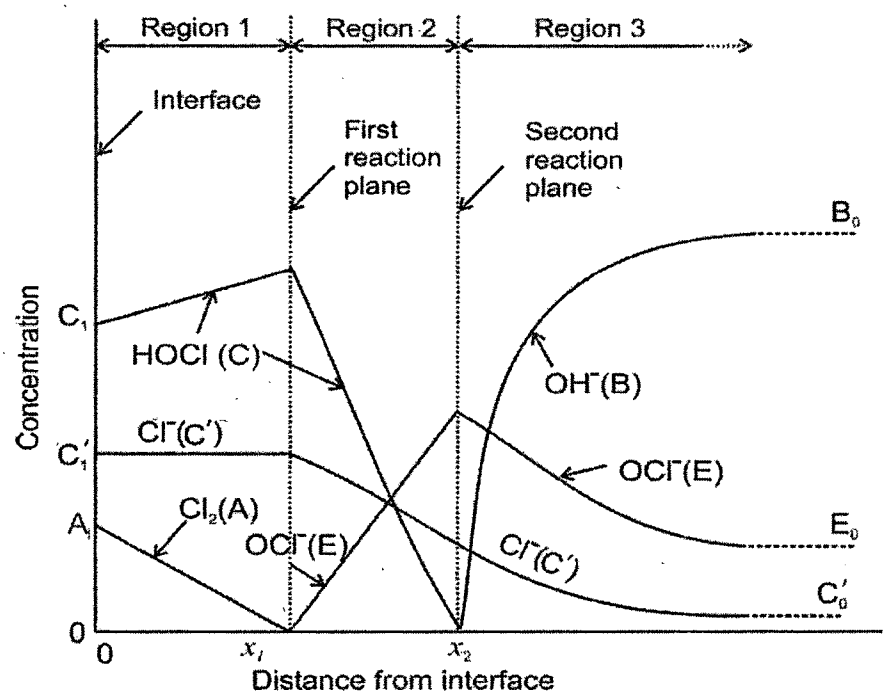

Figure 4.2.1: Concentration profiles for absorption of Cl_2 into aqueous $NaOH$ solution

Since, the equilibrium constant ratio $P = K_1/K_2 = 1.4 \times 10^4\ gmol/l$, is very high, so we can apply the two reaction plane model to the present system.

The diffusion coefficients of all species, based on the penetration theory is modeled by partial differential equations. The concentration profile for each species which will be derived by solving the developed model will be similar to that as shown in Figure 4.2.1.

Region 1 $(0 < x < x_1)$

$$D_A \frac{\partial^2 C_A}{\partial x^2} = \frac{\partial C_A}{\partial t} + r_1 \tag{4.2.17}$$

$$D_C \frac{\partial^2 C_C}{\partial x^2} = \frac{\partial C_C}{\partial t} + r_2 \tag{4.2.18}$$

Region 2 $(x_1 < x < x_2)$

$$D_C \frac{\partial^2 C_C}{\partial x^2} = \frac{\partial C_C}{\partial t} + r_2 \tag{4.2.19}$$

$$D_E \frac{\partial^2 C_E}{\partial x^2} = \frac{\partial C_E}{\partial t} + r_3 \tag{4.2.20}$$

Region 3 $(x_2 < x < \infty)$

$$D_B \frac{\partial^2 C_B}{\partial x^2} = \frac{\partial C_B}{\partial t} + r_4 \tag{4.2.21}$$

$$D_E \frac{\partial^2 C_E}{\partial x^2} = \frac{\partial C_E}{\partial t} + r_3 \tag{4.2.22}$$

with the following initial and boundary conditions:

$$t = 0, x > 0; C_B = C_{B0}, C_E = C_{E0} \tag{4.2.23}$$

$$x = 0, t > 0; C_A = C_{Ai}^*, \frac{\partial C_C}{\partial x} = 0, C_C = C_{C0} \tag{4.2.24}$$

$$x = x_1, t > 0; C_A = C_E = 0, 2D_A \frac{\partial C_A}{\partial x} = 2D_E \frac{\partial C_E}{\partial x} = D_C \frac{\partial C_C}{\partial x} \tag{4.2.25}$$

$$x = x_2, t > 0, C_B = C_C = 0, D_B \frac{\partial C_B}{\partial x} = -D_C \frac{\partial C_C}{\partial x} D_E \left[\left(\frac{\partial C_E}{\partial x} \right)_2 - \left(\frac{\partial C_E}{\partial x} \right)_3 \right] \tag{4.2.26}$$

$$x = \infty, t \geq 0; C_B = C_{B0}, C_E = C_{E0} \tag{4.2.27}$$

where x_1 and x_2 are the locations of the first and the second reaction planes, respectively, and $(\partial C_E/\partial x)_2$ and $(\partial C_E/\partial x)_3$ represent the values of $\partial C_E/\partial x$ when x approaches x_2 from region 2 and from region 3, respectively.

This proposed model is more general.

Specifically, when the effect of r_1, r_2, r_3 *and* r_4 are negligible and hence if removed from the equations, the proposed model will reduce to model of Hikita et al. (1973)

The analytical solution of this problem (i.e. concentration profile in the liquid) was given by Hikita et al. (1973) and is as follows:

Region 1 ($0 < x < x_1$)

$$C_A = C_{Ai}^* \left[1 - \frac{\text{erf}\,(x/2\sqrt{D_A t})}{\text{erf}\,(\sigma_1)}\right] \tag{4.2.28}$$

$$C_B = 0 \tag{4.2.29}$$

$$C_C = C_{B0}\sqrt{\frac{D_B}{D_C}}\exp\left[\left(\frac{D_A}{D_C} - \frac{D_A}{D_B}\right)\sigma_2^2\right] \tag{4.2.30}$$

$$\frac{\text{erf}\left(\sqrt{D_A/D_C}\,\sigma_2\right) - erf\left(\sqrt{D_A/D_C}\,\sigma_1\right)}{erf_c\left(\sqrt{D_A/D_B}\,\sigma_2\right)}$$

$$C_E = 0 \tag{4.2.31}$$

Region 2 ($x_1 < x < x_2$)

$$C_A = 0 \tag{4.2.32}$$

$$C_B = 0 \tag{4.2.33}$$

$$C_C = C_{B0}\sqrt{\frac{D_B}{D_C}}exp\left[\left(\frac{D_A}{D_C} - \frac{D_A}{D_B}\right)\sigma_2^2\right] \tag{4.2.34}$$

$$\frac{erf\left(\sqrt{D_A/D_C}\,\sigma_2\right) - \text{erf}\,(x/2\sqrt{D_C t})}{erf_c\left(\sqrt{D_A/D_B}\,\sigma_2\right)}$$

$$C_E = C_{Ai}^*\sqrt{\frac{D_A}{D_E}}exp\left[\left(\frac{D_A}{D_E} - 1\right)\sigma^2{}_1\right] \tag{4.2.35}$$

$$\frac{\text{erf}\,(x/2\sqrt{D_E t}) - erf\left(\sqrt{D_A/D_E}\,\sigma_1\right)}{erf(\sigma_1)}$$

Region 3($x_2 < x < \infty$)

$$C_A = 0 \tag{4.2.36}$$

$$C_B = C_{Bo}\frac{\text{erf}\,(x/2\sqrt{D_B t} - erf(\sqrt{D_A/D_B}\,\sigma_2)}{erf_c\,(\sqrt{D_A/D_B}\,\sigma_2)} \tag{4.2.37}$$

$$C_C = 0 \tag{4.2.38}$$

$$C_E = C_{Ai}^{*}\sqrt{\frac{D_A}{D_E}}exp\left[\left(\frac{D_A}{D_E}-1\right)\sigma_1^2\right] \tag{4.2.39}$$

$$\frac{erf(\sqrt{D_A/D_E}\,\sigma_2) - (\sqrt{D_A/D_E}\,\sigma_1)}{\text{erf}\,(\sigma_1)erf_c(\sqrt{D_A/D_E}\,\sigma_2)} \times erf_c(x/2\sqrt{D_E t})$$

$$+C_{E0}\frac{erf(x/2\sqrt{D_E t}) - erf(\sqrt{D_A/D_B}\,\sigma_2)}{erf_c(\sqrt{D_A/D_E}\,\sigma_2)}$$

Proposed mathematical model I: This model is represented by equations (4.2.17 – 4.2.27), when r_1, r_2, r_3 *and* r_4 are non zero.

Proposed mathematical model II: This model is represented by equations (4.2.17 – 4.2.22) when effect of r_1, r_2, r_3 *and* r_4 are negligible with modifying boundary conditions which are as follows:

$$t = 0, x > 0; C_B = C_{B0}, C_E = C_{E0} \tag{4.2.40}$$

$$x = 0, t > 0; C_A = C_{Ai}^{*}, \frac{\partial C_C}{\partial x} = 0, C_C = C_{C0} \tag{4.2.41}$$

$$x = x_1, t > 0; C_A = C_E = 0,$$

$$2D_A\frac{\partial C_A}{\partial x} = -2D_E\frac{\partial C_E}{\partial x} = 2D_C\frac{\partial C_C}{\partial x} = D_C\left[\left(\frac{\partial C_C}{\partial x}\right)_2 - \left(\frac{\partial C_C}{\partial x}\right)_1\right] \tag{4.2.42}$$

$$x = x_2, t > 0, C_B = C_C = 0, D_B\frac{\partial C_B}{\partial x} = -D_C\frac{\partial C_C}{\partial x} = D_E\left[\left(\frac{\partial C_E}{\partial x}\right)_2 - \left(\frac{\partial C_E}{\partial x}\right)_3\right] \tag{4.2.43}$$

$$x = \infty, t \geq 0; C_B = C_{B0}, C_E = C_{E0} \tag{4.2.44}$$

In proposed mathematical model II, we have consider the effect of jump at $x = x_1$ and $x = x_2$. The two plane model theory suggest us that at $x = x_1$ there is a instantaneous

reaction between species $A(Cl_2)$ and $E(OCl^-)$ and causes jump in concentration of species C $(HOCl)$. Similarly, at $x = x_2$ there is a sudden reaction between species C $(HOCl)$ and B (OH^-) and causes jump in concentration of species E (OCl^-). This jump values are defined by the last term of the Equation (4.2.42) and Equation (4.2.43) respectively.

The absorption rate for proposed mathematical model I can be calculated by equation (4.2.11) and

$$\beta = \frac{1}{\mathrm{erf}(\sigma_1)} \tag{4.2.45}$$

where the constant σ_1 can be determined by solving the following pair of simultaneous equations.

$$\frac{C_{C0}}{C_{Ai}^*}\sqrt{\frac{r_2 D_C}{r_1 D_A}} = \frac{C_{B0}}{C_{Ai}^*}\sqrt{\frac{r_4 D_B}{r_1 D_A}} \times \frac{exp\left[\left(\frac{r_1 D_A}{r_2 D_C} - \frac{r_1 D_A}{r_4 D_B}\right)\sigma_2^2\right] erf\left[\left(\sqrt{\frac{r_1 D_A}{r_2 D_C}}\right)\sigma_2\right]}{erf_c\left[\left(\sqrt{\frac{r_1 D_A}{r_4 D_B}}\right)\sigma_2\right]}$$

$$- \frac{2exp\left[\left(\frac{r_1 D_A}{r_2 D_C} - 1\right)\sigma_1^2\right] erf\left[\sqrt{\left(\frac{r_1 D_A}{r_2 D_C}\right)}\sigma_1\right]}{\mathrm{erf}\,(\sigma_1)} \tag{4.2.46}$$

$$\frac{C_{E0}}{C_{Ai}^*}\sqrt{\frac{r_3 D_E}{r_1 D_A}} = \frac{C_{B0}}{C_{Ai}^*}\sqrt{\frac{r_4 D_B}{r_1 D_A}} \times \frac{exp\left[\left(\frac{r_1 D_A}{r_3 D_E} - \frac{r_1 D_A}{r_4 D_B}\right)\sigma_2^2\right] erf\left[\left(\sqrt{\frac{r_1 D_A}{r_3 D_E}}\right)\sigma_2\right]}{erf_c\left[\left(\sqrt{\frac{r_1 D_A}{r_4 D_B}}\right)\sigma_2\right]}$$

$$- \frac{2exp\left[\left(\frac{r_1 D_A}{r_3 D_E} - 1\right)\sigma_1^2\right] erf\left[\sqrt{\left(\frac{r_1 D_A}{r_3 D_E}\right)}\sigma_1\right]}{\mathrm{erf}\,(\sigma_1)} \tag{4.2.47}$$

Similarly the absorption rate for proposed mathematical model II can be calculated by equation (4.2.11) and

$$\beta = \frac{1}{\mathrm{erf}(\sigma_1)} \tag{4.2.48}$$

where the constant σ_1 can be determined by solving the following pair of simultaneous equations.

$$\frac{C_{C0}}{C_{Ai}^*}\sqrt{\frac{D_C}{D_A}} = \frac{C_{B0}}{C_{Ai}^*}\sqrt{\frac{D_B}{D_A}} \times \frac{exp\left[\left(\frac{D_A}{D_C} - \frac{D_A}{D_B}\right)\sigma_2^2\right] erf\left[\left(\sqrt{\frac{D_A}{D_C}}\right)\sigma_2\right]}{erf_c\left[\left(\sqrt{\frac{D_A}{D_B}}\right)\sigma_2\right]}$$

$$- \frac{2exp\left[\left(\frac{D_A}{D_C} - 1\right)\sigma_1^2\right] erf\left[\sqrt{\left(\frac{D_A}{D_C}\right)}\sigma_1\right]}{\text{erf}\,(\sigma_1)} \qquad (4.2.49)$$

$$\frac{2C_{E0}}{C_{Ai}^*}\sqrt{\frac{D_E}{D_A}} = \frac{C_{B0}}{C_{Ai}^*}\sqrt{\frac{D_B}{D_A}} \times \frac{exp\left[\left(\frac{D_A}{2D_E} - \frac{D_A}{D_B}\right)\sigma_2^2\right] erf\left[\left(\sqrt{\frac{D_A}{2D_E}}\right)\sigma_2\right]}{erf_c\left[\left(\sqrt{\frac{D_A}{D_B}}\right)\sigma_2\right]}$$

$$- \frac{exp\left[\left(\frac{D_A}{2D_E} - 1\right)\sigma_1^2\right] erf\left[\sqrt{\left(\frac{D_A}{2D_E}\right)}\sigma_1\right]}{\text{erf}\,(\sigma_1)} \qquad (4.2.50)$$

The equations (4.2.45), (4.2.46) (4.2.47) (4.2.48) (4.2.49) and (4.2.50) are solved by the trial and error procedure based on Newton – Raphson technique to evaluate σ_1 and σ_2 . In this technique the first guess values of σ_1 and $\sigma_2$was calculated by considering equal diffusivities i.e. $D_A = D_B = D_C = D_E$.

There are several numerical methods like finite difference method, finite volume method, finite element method etc. to solve proposed mathematical model I and proposed mathematical Model II. Looking to the nature of the mathematical model (time dependent and in one dimension) FDM is the best suitable technique. Other methods are expensive from time point of view. Hence, we have used the numerical technique, finite difference method, to solve the model using Matlab software.

4.2.3 Results and discussion

The effect of the diffusivity ratio on enhancement factor

Figure 4.2.2 shows the plot of the enhancement factor β versus the concentration ratio C_{B0}/C_{Ai}^* for different diffusivities ratio of D_B/D_A with constant D_C/D_A and D_E/D_A. The

value of D_B/D_A are taken 2.43, 1 and 0.1. In this figure the plots of Hikita (1972), proposed mathematical model I [equations (4.2.17 – 4.2.27) with $r_1, r_2, r_3 and\ r_4$ are non zero] and proposed mathematical model II [equations (4.2.17 – 4.2.22 and 4.2.40 – 4.2.44) with $r_1, r_2, r_3\ and\ r_4$ are zero] are presented.

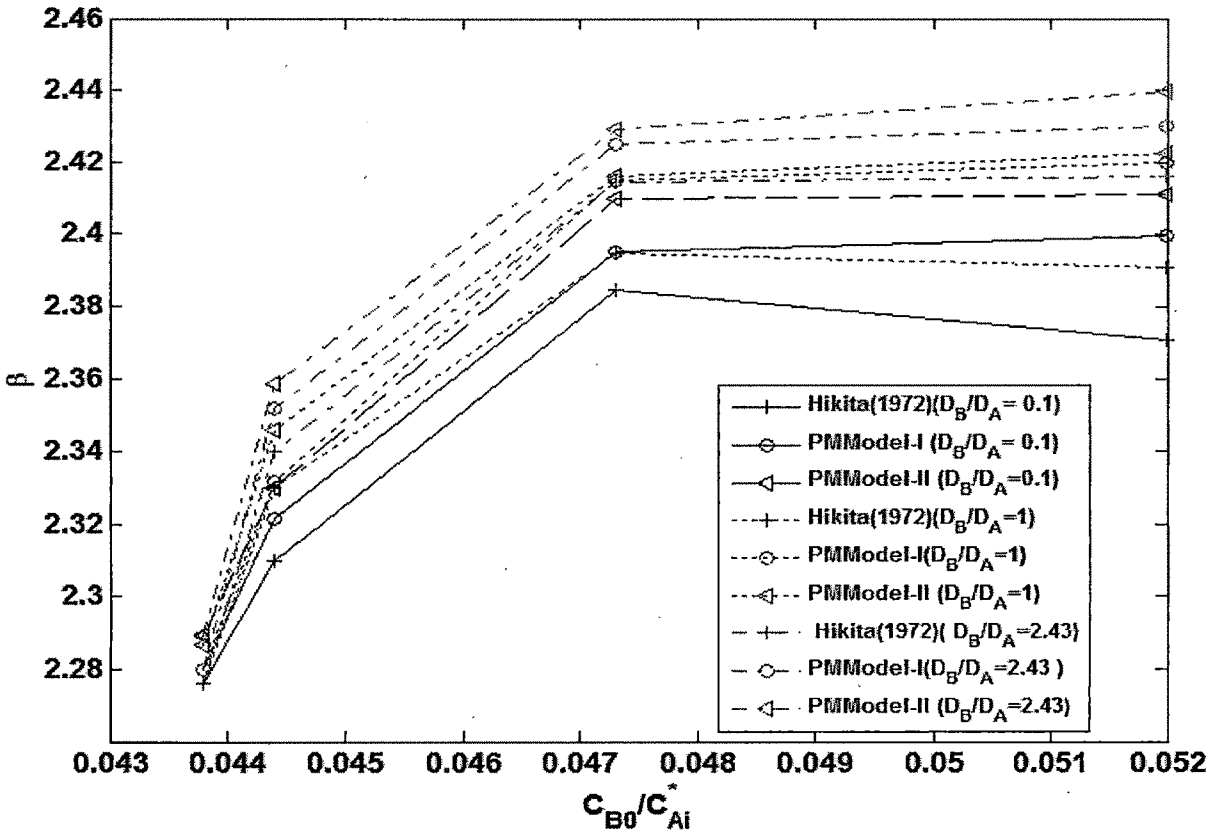

Figure 4.2.2 : Variation in enhancement factor with respect to C_{B0}/C^*_{Ai} at different $D_B/D_A = 2.43, 1, 0.1$ and constant $D_E/D_A = 10$ and $D_C/D_A = 0.1$ for absorption of Cl_2 into aqueous $NaOH$ solution

The following results may be drawn from figure (4.2.2).

- The lines in the figure having higher D_B/D_A are at higher position for the same C_{B0}/C^*_{Ai}. This indicates that at higher ratio of diffusivities of reactants (liquid and gas), the enhancement factor is higher. It can be concluded that higher the diffusivity of liquid reactant with respect to gaseous reactant, higher is the enhancement factor. The increase in enhancement factor is due to reduction in thickness of interfacial film. The reduction in thickness in interfacial film is due to movement of reactant $B\ (NaOH)$ is faster toward interface compared to movement of $A\ (Cl_2)$ toward bulk of liquid.

- For same D_B/D_A plots shows that enhancement factor increases with increase in the reactant ratio (C_{B0}/C_{Ai}^*). The increase in enhancement factor is steeper at initial increase of C_{B0}/C_{Ai}^*. After that the rate of rise in enhancement factor with respect to rate of rise in reactant ratio is reducing and after certain value of C_{B0}/C_{Ai}^*, there is hardly any rise is enhancement factor with respect to reactant ratio. It can be concluded that there is increase in enhancement factor with increase in liquid reactant concentration up to certain limits. This may be taken to mean that at higher C_{B0} enhancement factor is higher. The reduction of β at higher C_{B0}/C_{Ai}^* is due to high viscosity of $NaOH$ solution at higher C_{B0}.

- For the same ratio of C_{B0}/C_{Ai}^* the value of enhancement factor derived from proposed mathematical model II is higher than the value from proposed mathematical model I. The value derived from Hikita (1972) is the lowest. The predicted values from proposed mathematical model I and proposed mathematical model II are higher than Hikita (1972) as the effect of $HOCl$ diffusing out have been considered.

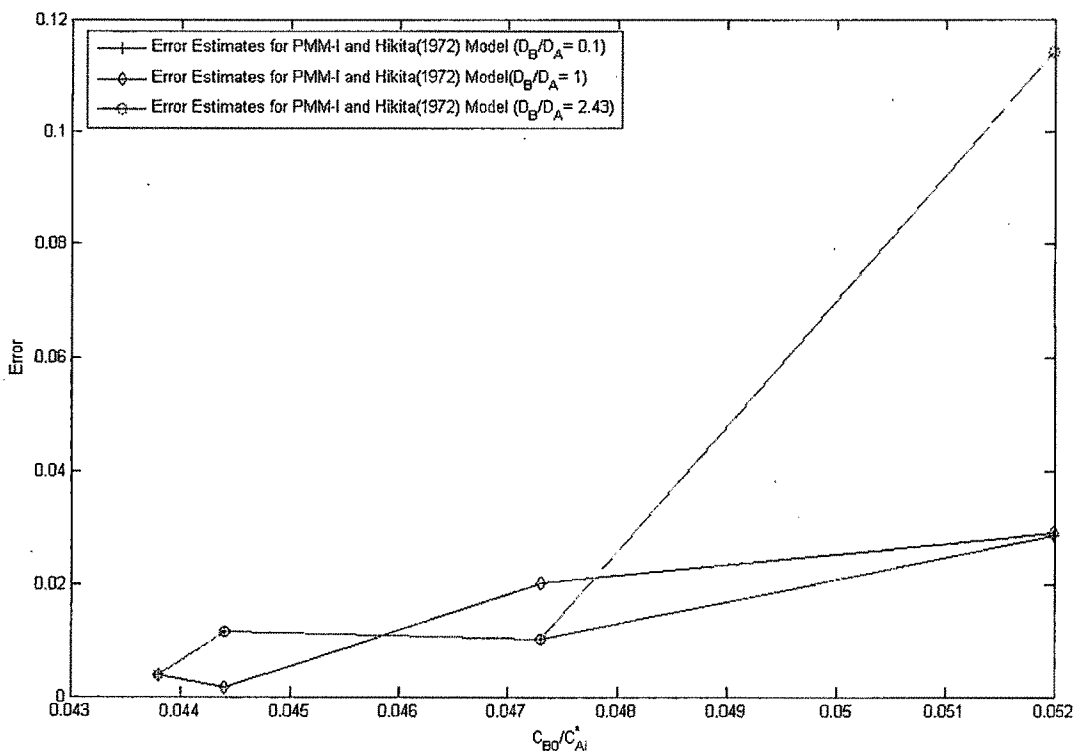

Figure 4.2.3 : Error estimates between experimental data and proposed mathematical model at different $D_B/D_A = 2.43, 1, 0.1$ and constant $D_E/D_A = 10$ and $D_C/D_A = 0.1$.

Figure 4.2.3 shows the error estimates between Hikita (1972) model and proposed mathematical model I. Here error is defined as follow:

$Error = |\beta \text{ predicted by Hikita (1972) model} - \beta \text{ predicted by proposed model I}|$

for diffusivities $D_B/D_A = 2.43,\ 1,0.1$

It is observed that the lower value of D_B/D_A for different C_{B0}/C_{Ai}^*, the proposed mathematical model I and Hikita (1972) model are comparable. However, for higher values of D_B/D_A, the comparison shows that there is a numerical instability in Hikita (1972) model (higher value of error). Therefore, we conclude that the proposed model I is well-posed.

Comparison of experimental results with simulated results

Figure (4.2.4) is a comparison of β predicted by the simulated results of Hikita (1973), proposed mathematical model I and proposed mathematical model II with experimentally determined values (for $C_{Ag,in} = 0.602\ x\ 10^{-3}\ kmol/m^3$) at actual value of diffusivity ratio: $D_B/D_A = 2.32, D_C/D_A = 1.04, D_{C'}/D_A = 1.4$ and $D_E/D_A = 0.786$ (Table A 3.4). It may be observed that the values obtained by experiment, Hikita (1973) model and proposed model I are comparable. Equations (4.2.17) to (4.2.22) and (4.2.45) to (4.2.50) indicate that β is a function of rate of reactions and three diffusivity (in liquid) ratios, D_B/D_A D_C/D_A and D_E/D_A. The predicted values by proposed mathematical model I are higher to some extent than Hikita (1973) model which is due to the effect of reaction on β, have been consider in mathematical model I. It may be make out that the influence of rate of reaction are marginal that may be because being instantaneous reaction diffusivity ratio of species are rate controlling.

$C_{B0}, kmol/m^3$	0.95	0.75	0.525	0.031
Exp. value of β for $C_{Ag,in} = 0.602\ x\ 10^{-3}\ kmol/m^3$	1.55	1.5	2.24	1.94

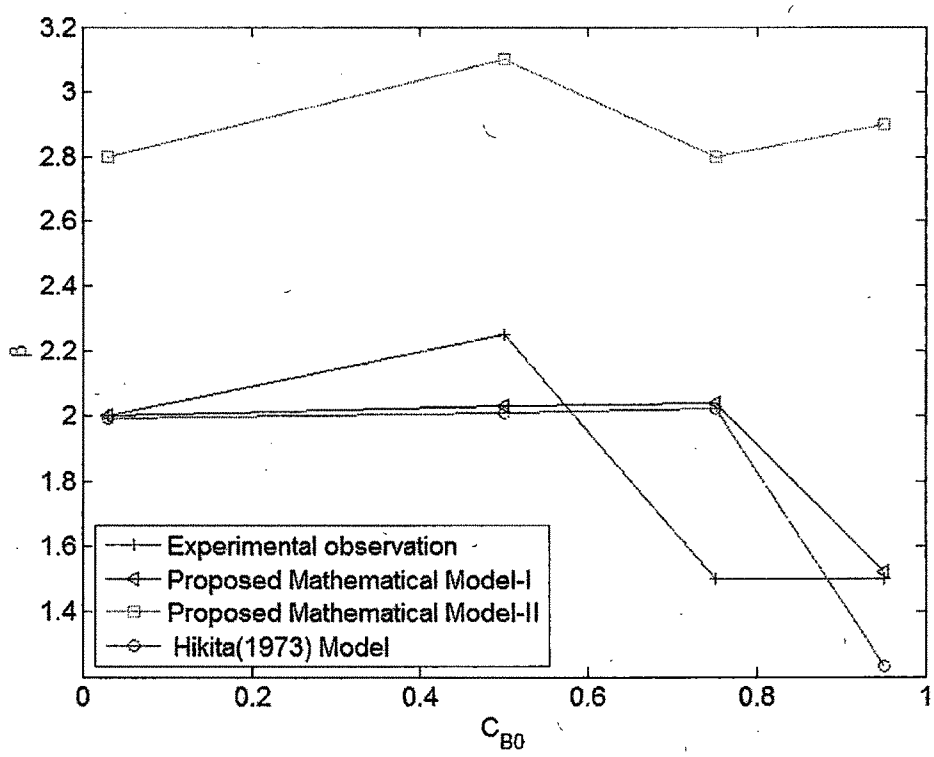

Figure 4.2.4 : Comparison of value of β determined experimentally and by proposed mathematical model for different C_{B0} at $C_{Ag,in} = 0.602\ x\ 10^{-3}\ kmol/m^3$

The values predicted by proposed mathematical model II for β are higher than experimental values. It may be concluded that the effect of jumping in the concentration of $HOCl$ and OCl^- which have been considered in the model at the interface 1 and 2 are not appreciable. Hence the values predicted by model II are higher. So model II is not appropriate under operating conditions of the experiment.

4.2.4 Conclusion

- The enhancement factor depends on the five independent dimensionless parameters i.e., three diffusivity ratios, D_B/D_A D_C/D_A and D_E/D_A, and two concentration ratios C_{B0}/C_{Ai}^* and E_0/C_{Ai}^*.
- The enhancement factor increases as the value of D_B with respect to D_A increases.
- The value of enhancement factor increases as the value C_{B0} increases, and the effect of C_{B0}/C_{Ai}^* becomes large at low values and low at high values C_{B0}/C_{Ai}^*
- The proposed mathematical model I is more appropriate to experimental results at operating conditions i.e. at 30^0C.

4.3 Numerical model of rate of absorption in multi nozzle jet ejector (chlorine- aqueous $NaOH$ solution)

High velocity jet from the nozzles entrains the gas and due to very high turbulence in the throat, gas is split into bubbles. In the diffuser section partial separation of the gas and liquid may occur. The high interfacial area formed by bubbles is desirable for increasing rate of mass transfer. Different researchers, including Kuznetsov and Oratovskii (1962), Boyadzhiev (1964), Volgin et al. (1968) and Beg and Taheri (1974), attempted to simulate the operation of the jet ejector for gas absorption.

Johnstone et al. (1954) reported a jet ejector study in which SO_2 was absorbed in $0.6N$ $NaOH$ solution, and the amount of sulfur dioxide absorbed in the liquid, was measured at various distances from the point of liquid injection. It was found that the mass transfer increased substantially as the liquid injection rate increased.

Kuznetsov and Oratovskii (1962) developed a mathematical model for predicting absorption of CO_2 by reacting with $NaOH$ solution in the throat and the divergent section of a venturi scrubber.

SO_2 removal efficiency of a jet ejector was investigated by Talaie et al. (1997) using a three-dimensional mathematical model based on a non uniform droplet concentration distribution predicted from a dispersion model in the gas flow where the gas-phase mass transfer coefficient was calculated by empirical equations.

Mandal et al (2003) studied the jet ejector followed by bubble column and developed two simple correlations of a and $k_L a$ as a function of superficial gas velocity. This correlation can be combined to calculate liquid-side mass transfer coefficient k_L.

Utomo et al. (2008) investigated the influence of operating conditions and ejector geometry on the hydrodynamics and mass transfer characteristics of the ejector by using three-dimensional CFD modeling. The CFD results were validated with experimental data.

Taheri et al. (2010) studied the three-dimensional mathematical model, based on annular two-phase flow model for the prediction of the amount of SO_2 removed in a venturi scrubber.

Author has made an attempt to predict mass transfer characteristics by numerical modeling. Here, the author has described the mathematical model for the prediction of the amount of

chlorine removed in jet ejector. The results of simulation are compared with the experimental data.

4.3.1 Mathematical modeling

In this study the model developed by Taheri et al. (2010) is modified to suit the jet ejector used in the present work. Taheri et al. (2010) developed a three-dimensional mathematical model based on annular two-phase flow model in rectangular geometry of the venturi scrubber. They develop a model to predict interfacial area by predicting drop size and droplet concentration. Instead in this work an attempt is made to predict the change in concentration of reactant, A, through the ejector.

The concentration of bubbles has been assumed uniform across the cross section of the scrubber.

For developing the model, the pollutant concentration distribution in gas phase was obtained by the following model using mass balance.

The general equation can be obtained by writing differential mass balance for pollutants over a differential control volume.

The rate of reaction of pollutant A per unit volume at time t for constant volume system may be written as

$$r_A = -\frac{dC_{Ag}}{dt}$$

The r_A may be calculated by using rate of mass transfer per unit area as

$$-r_A = N_A a$$

where a = interfacial area per unit volume

= (number of bubble / volume) x (interfacial area / bubble)

$= C_b(\pi D_b^2)$

dt may be computed from velocity in case of moving gas as $\frac{dZ}{dv_G}$

∴ equation (4.3.1) may be written as

$$\frac{d(v_G C_{Ag})}{dZ} = -N_A(\pi\, {D_b}^2)C_b \qquad (4.3.1)$$

Boundary conditions for Equation (4.3.1) are as follows:

$$Z = 0;\ C_{Ag} = C_{Ag,in} \qquad (4.3.2)$$

The value of D_b may be estimated by using the following equation (Ogawa et al., 1983)

$$D_b = 1.213\ x\ 10^{-2} v_{G,S}^{0.2} \left(\frac{v_{L,th}^2}{gD_T}\right) \qquad (4.3.3)$$

Substituting equation (4.3.3) in equation (4.3.1) it will reduce to

$$\frac{d(v_G C_g)}{dZ} = -N_A\pi \left[1.213\ x\ 10^{-2} v_{G,S}^{0.2} \left(\frac{v_{L,th}^2}{gD_T}\right)\right]^2 C_b \qquad (4.3.4)$$

In order to evaluate the bubble concentration distribution, C_b, in the above equations, the following one-dimensional dispersion equation, expressing material balance for bubble in a differential control volume, must be solved:

$$\frac{d(v_b C_b)}{dZ} = S\,(0.0024n^3 - 0.0309n^2 + 0.1108n + 0.5156) \qquad (4.3.5)$$

with the boundary conditions of:

$$Z = 0;\ v_b C_b = 0 \qquad (4.3.6)$$

where n is a number of nozzle (orifice). The expression for n have been determined by using multi regression to suit the experimental result.

In equation (4.3.3), the bubbles are convected in the Z direction.

It is assumed that for each nozzle the source of bubbles is limited to one element. The source strength, S, is the number of bubbles generated per unit volume per unit time. Bubbles are carried from element to element and are dispersed by convection and eddy diffusion effects. Number of bubbles per second is defined by the following equation:

$$N_b = \frac{G}{\left(\frac{\pi}{6}\right) {D_b}^3} = S \qquad (4.3.7)$$

where G is the total gas flow rate.

Substituting equation (4.3.3) and (4.3.7) in equation (4.3.4) it will reduce to

$$\frac{d(v_b C_b)}{dZ} = \frac{G}{\left(\frac{\pi}{6}\right) {D_b}^3} = \frac{G}{\frac{\pi}{6}\left[1.213\, x\, 10^{-3} u_G^{0.2} \left(\frac{v_{L,th}^2}{g D_T}\right)\right]^3} \tag{4.3.8}$$

$$\therefore \quad C_b \frac{d(v_b)}{dZ} = v_b \frac{d(C_b)}{dZ} = \frac{G}{\frac{\pi}{6}\left[1.213\, x\, 10^{-3} u_G^{0.2} \left(\frac{v_{L,th}^2}{g D_T}\right)\right]^3} \tag{4.3.9}$$

The bubble velocity can be obtained by solving the following equation. This is obtained by writing a force balance for bubbles.

$$\frac{dv_b}{dZ} = \frac{3\mu_l (v_l - v_b) C_{DN}}{4\rho_g {D_b}^2 v_b} \tag{4.3.10}$$

The modified drag coefficient, C_{DN}, can be calculated by using the following expressions given by Taheri et al. (2010) adopted for bubbles:

$$C_{DN} = C_D Re_b \tag{4.3.11}$$

$$C_D = C_{Dl} \left(\frac{v_l}{v_l - v_b}\right)^{0.5} \tag{4.3.12}$$

Here C_{Dl} can be obtained by the formula given by Tahari et al. (2010) adopted for bubbles:

$$C_{Dl} = 0.22 + \frac{24}{Re_g} \left(1 + 0.15\, {Re_g}^{0.6}\right) \tag{4.3.13}$$

Substituting Equation (4.3.11) (4.3.12) and (4.3.13) in Equation (4.3.10) it will reduce to

$$\frac{dv_b}{dZ} = \frac{3\mu_l (v_l - v_b)}{4\rho_g {D_b}^2 v_b} C_D Re_b \tag{4.3.14}$$

$$\therefore \quad \frac{dv_b}{dZ} = \frac{3\mu_g (v_l - v_b)}{4\rho_l {D_b}^2 v_b} C_{Dl} \left(\frac{v_l}{v_g - v_B}\right)^{0.5} Re_b \tag{4.3.15}$$

$$\therefore \quad \frac{dv_b}{dZ} = \frac{3\mu_g (v_l - v_b)}{4\rho_l {D_b}^2 v_b} \left[0.22 + \frac{24}{Re_g} \left(1 + 0.15\, {Re_g}^{0.6}\right)\right] \left(\frac{v_l}{v_g - v_B}\right)^{0.5} Re_b \tag{4.3.16}$$

The gas velocity is computed by the following equation:

$$v_g = \frac{G}{\left(\frac{G}{G+L}\right)\frac{\pi}{4}D_T^2} \tag{4.3.17}$$

The equation (4.3.1) can be solved simultaneously with equation (4.3.3), (4.3.5), (4.3.7), (4.3.9), (4.3.16) and (4.3.17).

The mass transfer rate N_A, in each element can be evaluated by model developed in previous section presented by equation 4.1.32.

When pollutants undergo a very fast reaction into the liquid phase such as absorption of Cl_2 into aqueous $NaOH$ solution, the bulk concentration of gas in the liquid phase can be considered equal to zero.

4.3.2 Results and discussions

Figure 4.3.1 is a plot of variation of gas phase concentration C_{Ag} along the axis of ejector for different values of initial gas concentration for nozzle N1 having number of orifice1. For comparison of the experimental results and predicted results obtained by the proposed model are plotted in the same figure. From both the profiles shown in the figure, it is clear that the proposed model is in good agreement with experimental results.

Figure (4.3.2) shows the variation of gas phase concentration C_{Ag} along the axis of the ejector for different nozzles N5 (no. of orifice 1), N6 (no. of orifice 3) and N7 (no. of orifice 5). The results predicted by the model are in good agreement with the experimental results. Thus the model is applicable for multi nozzle jet ejector.

It is also shows that the conversion in the jet ejector first increases then decreases and finally becomes almost constant. The number of orifice in the nozzle affects the gas conversion in the jet ejector with three orifice (N6) the conversion obtained is maximum with five orifice (N7) minimum and with one orifice (N5) in between maximum and minimum.

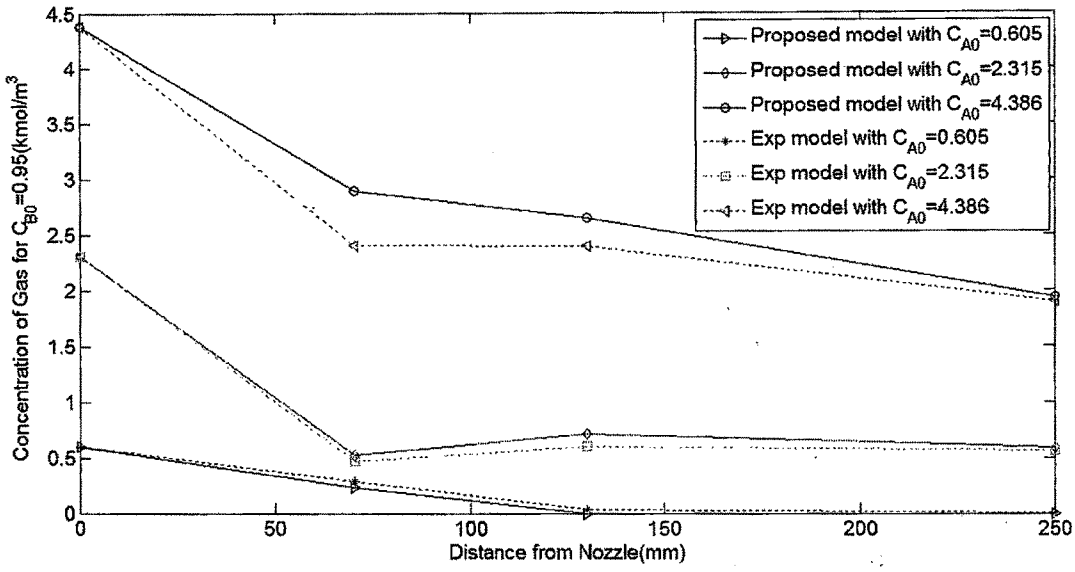

Figure 4.3.1 : Variation of gas phase concentration C_{Ag} along the axis of ejector for different values of initial gas concentration $C_{Ag,in}$ at $C_{B0} = 0.95\ kmol/m^3$ (comparison between proposed model and experimental value)

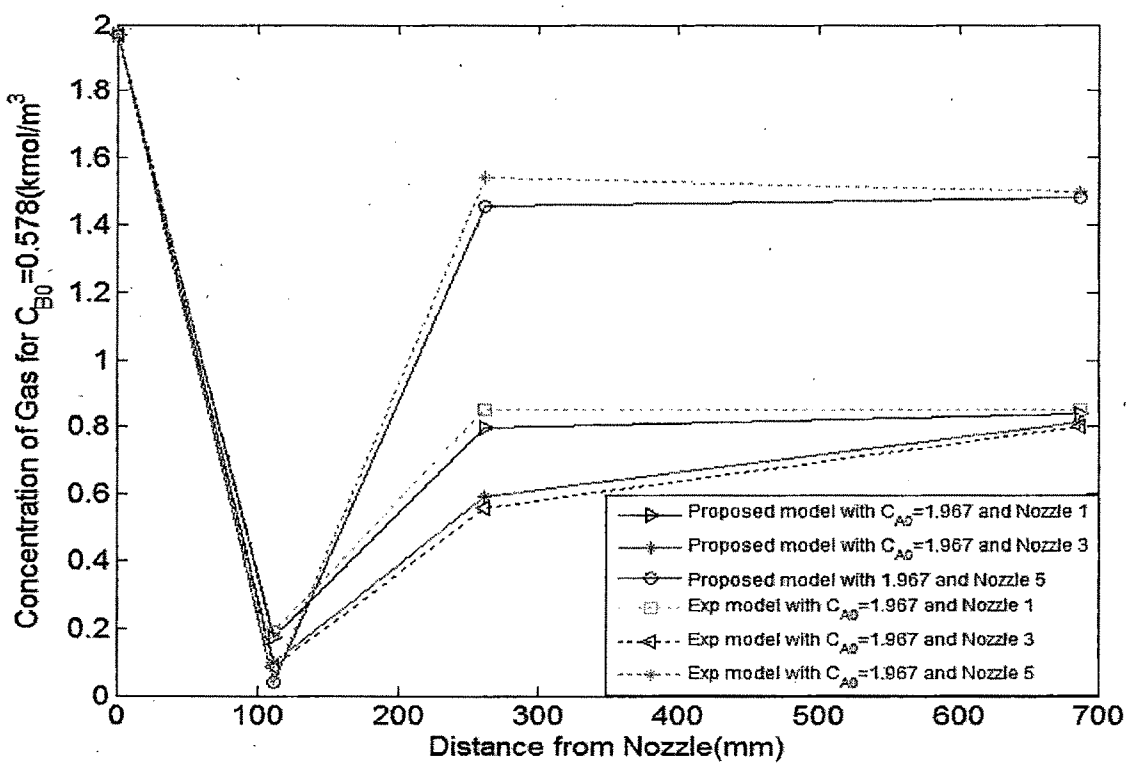

Figure 4.3.2 : Variation of gas phase concentration C_{Ag} along the axis of ejector for different nozzles N5 (no. orifice 1), N6 (no. of orifice 3) and N7 (no. of orifice 5) for setup 3 at $C_{B0} = 0.578\ kmol/m^3$ and initial gas concentration $C_{Ag,in} = 1.967 \times 10^{-3}\ kmol/m^3$ (comparison between proposed model and experimental value)

The figure (4.3.3) shows the variation of bubble velocity along the axis of the ejector. It indicates that the bubble velocity suddenly increases to a maximum value and then it remains constant.

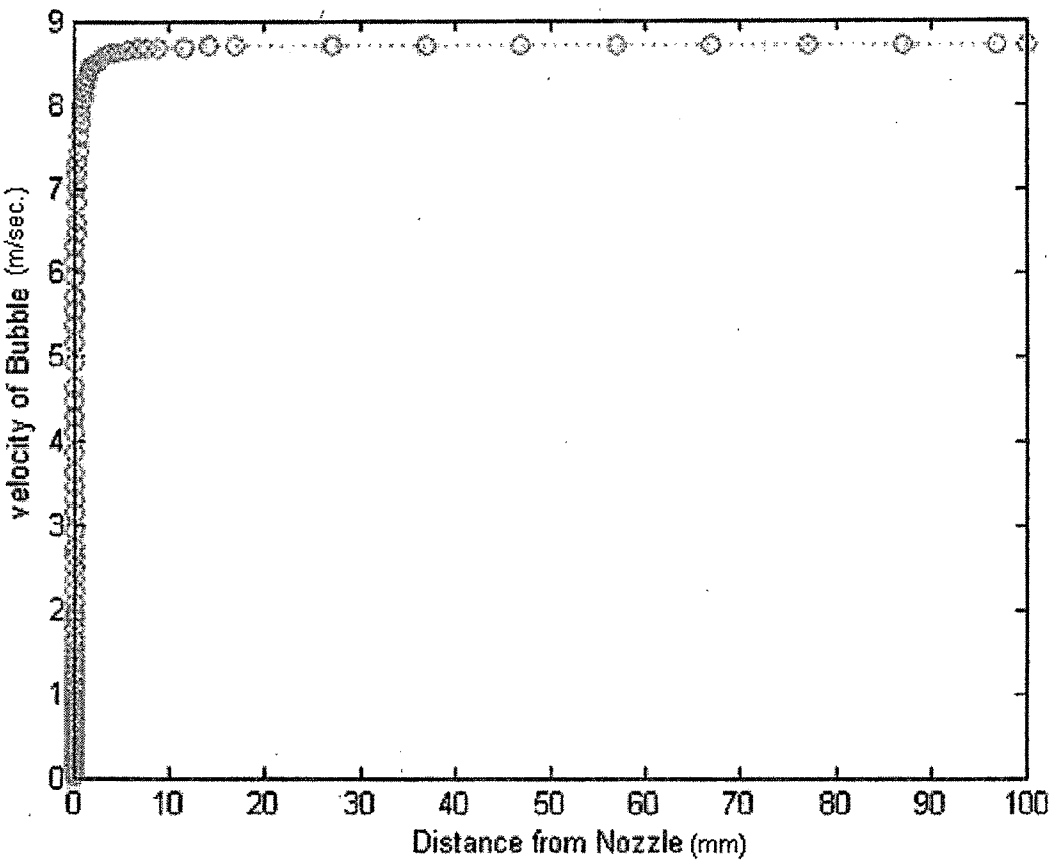

Figure 4.3.3 : Velocity profiles (m/sec.) of gas and droplet along axial direction (mm)

4.3.3 Conclusion

- The proposed model is in good agreement with experimental values for single nozzle as well as for multi nozzles. Hence the proposed model may be used for designing the industrial ejectors.
- The number of nozzle (orifice) affects the gas conversion. In present work the maximum conversion is obtained for no. of nozzle 3 (N6).

4.4 Mass transfer characteristics in multi nozzle jet ejector

In this section a mathematical model to predict hold up, mass transfer coefficient and interfacial area has been proposed for multi nozzle jet ejector and compared with experimental data obtained.

Many researchers have published their work on jet ejectors (Jackson, 1964; Volmuller and Walburg, 1973; Nagel et al., 1970; Hirner and Blenke, 1977; Zehner, 1975; Pal et al., 1980; Ziegler et al., 1977) because of the high energy efficiency in gas liquid contacting.

The kinetic energy of a high velocity liquid jet is used for getting fine dispersion and intense mixing between the phases in the jet ejectors.

Zlokamik, (1980) has reported that oxygen absorption efficiency is as high as 3.8 kg O_2/kwh in ejectors as compared to 0.8 kg O_2/kwh in a propeller mixer. The higher gas dispersion efficiency of the ejector type can be understood from the well known fact : "gas dispersion is possible only if the fraction of micro turbulence is high" (Schugerl, 1982).

Radhakrishnan et al. (1984) have used a vertical column fitted with a multi jet ejector for gas-dispersion for studying the pressure drop, holdup and interfacial area.

Agrawal (1999) has reported about 13000 m^2/m^3 interfacial area in horizontal single nozzle jet ejector. The range of measured values of the interfacial area in the jet ejector is about 3000 to 13000 m^2/m^3.

4.4.1 Hold up

Yamashita and Inoue (1975), Koetsier et al. (1976) and Mandal et al. (2004) reported the holdup characteristics with respect to gas flow rate in the jet ejector. At lower range of gas flow rate, gas hold up increases with increase in gas flow rate but at higher range of gas flow rates the increase in gas flow rate decreases the gas hold up or it remain constant depending on the height of liquid in the follow up column is high or low respectively. At lower gas flow rates small bubbles produced are in large number and at higher gas flow rate due to coalescence the bubbles of larger size are produced which lead to decrease in number of bubbles.

Hills (1976) has reported that the holdup is not affected by liquid flow rate. Mandal et al. (2004) observed that for the same gas flow rate the increase in liquid flow rate decreases the gas hold up.

The variables A_R, n, Re_{ls} and Re_{gs} affect the liquid holdup in a jet ejector.

Radhakrishnan et al. (1984) obtained following correlation by applying multi linear regressions analysis on their experimental data:

$$\chi_1 = 1 - \exp\left[-38.176\, {A_R}^{-0.06} n^{-0.06} {Re_{ls}}^{0.0002} {Re_{gs}}^{-0.55}\right] \qquad (4.4.1)$$

A new mathematical model has been attempted to predict the gas hold up as follows:

It is assumed that the model is of the form:

$$\alpha_1 = 1 - \exp\left[a_1 A_R^b n^c Re_{ls}^d Re_{gs}^e\right]$$

Therefore $\log[-\log(1-\alpha_1)] = \log a_1 + b_1 \log A_R + b_2 \log n + b_3 \log Re_{ls} + b_4 \log Re_{gs}$.

Using experimental data and multi linear regression analysis the values of a_1, b, c, d and e were obtained. The values obtained are $a_1 = -51.467$, $b = -0.03$, $c = 0.03$, $d = 0.0002$ and $e = -0.41$.

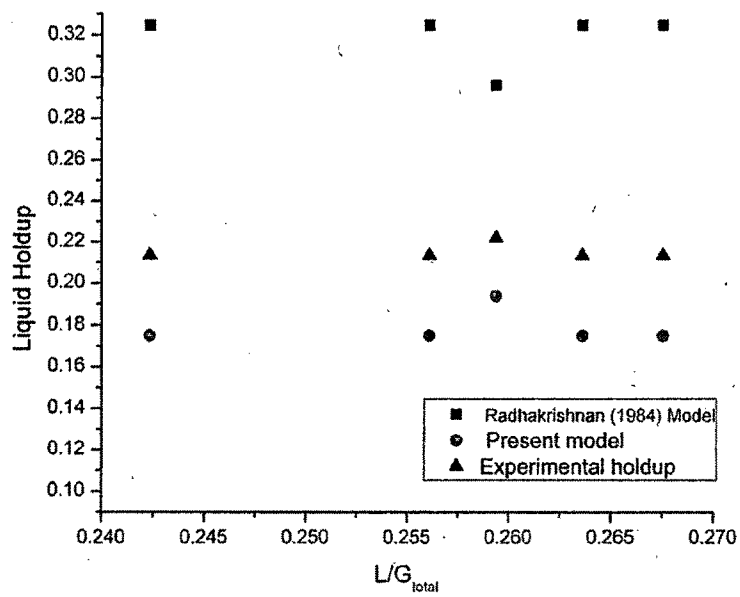

Figure 4.4.0 : Comparison of liquid holdup predicted by Radhakrishnan (1984), present model and experimental value at different L/G_{total} ratio.

Thus mathematical model for gas hold up is as follows.

$$\alpha_1 = 1 - \exp\left[-51.467\, A_R{}^{-0.03} n^{-0.03} Re_{ls}{}^{0.0002} Re_{gs}{}^{-0.41}\right] \qquad (4.4.2)$$

Liquid holdup may be determined by following equation.

$$\chi_1 = 1 - \alpha = \exp\left[-51.467\, A_R{}^{-0.03} n^{-0.03} Re_{ls}{}^{0.0002} Re_{gs}{}^{-0.41}\right] \qquad (4.4.3)$$

The results predicted from Radhakrishnan (1984) model and present model (equation – 4.4.3) is compared with actual experimental value at different L/G in figure (4.4.0).

4.4.2 New model to predict mass transfer characteristics, k_g and a

To predict mass transfer characteristics the value of k_G and a are required to be predicted. Here a mathematical model is developed to predict the value of k_G and a using chlorine-aqueous sodium hydroxide solution.

Doraiswamy and Sharma (1984) have reported that if

$$\frac{[D_A k_2 C_{OH}^0]^{1/2}}{k_L} > 3 \qquad (4.4.4)$$

and

$$\frac{[D_A k_2 C_{OH}^0]^{1/2}}{k_L} \ll \frac{C_{OH}^0}{2C_A^*} \qquad (4.4.5)$$

then the reaction is considered to be pseudo first order and in the fast reaction regime.

As absorption of Cl_2 in aqueous solution of $NaOH$ studied in the present work satisfy the condition (4.4.4) and (4.4.5), it is treated as pseudo first order fast reaction.

Levenspiel (1999) presented a simplified solvable pseudo first order rate expression as a replacement for second order reaction rate equation when the value of C_{B0} is so high that it do not change appreciably, which is presented here as follows:

$$-r_A dV = \frac{1}{\frac{1}{k_G a} + \frac{H_e}{a\sqrt{D_A k_2 C_{B0}}}} p_A . dV \qquad (4.4.6)$$

Now,

$$G'_{mo} = G_{mo}\,(1-y)$$

$$-r_A = -d(G_{mo}y) = -d\left(\frac{G'_{mo}y}{1-y}\right) = \frac{G'_{mo}dy}{(1-y^2)} \tag{4.4.7}$$

and

$$p_A = H_e C_A^* = yP \tag{4.4.8}$$

Substituting equation (4.4.7) and (4.4.8) in equation (4.4.6) we have:

$$\frac{G'_{mo}dy}{(1-y^2)} = \frac{1}{\frac{1}{k_g a} + \frac{H_e}{a k_{LR}}} yP.dV \tag{4.4.9}$$

where $k_{LR} = \sqrt{D_A k_2 C_{B0}}$

By rearranging equation (4.4.9) and integrating between $V = 0\ to\ V_R$ will yield the equation:

$$K_g = \frac{G'_{mo}}{P\,aV_R}\, ln\left[\frac{1-y_0}{y_0}\,\frac{y_i}{1-y_i} + \frac{1}{(1-y_i)^3} - \frac{1}{(1-y_0)^3}\right] \tag{4.4.10}$$

where,

$$\frac{1}{K_g} = \frac{1}{k_g} + \frac{H_e}{k_{LR}} \tag{4.4.11}$$

Interfacial area

Sharma and Danckwerts, (1970) stated that when

$$k_g.He \gg k_{LR} \tag{4.4.12}$$

Then gas phase resistance is negligible.

But for chlorine-aqueous $NaOH$ system

$$k_g.He \not\gg k_{LR}$$

Hence, to predict interfacial area few experiments were carried out for CO_2-aqueous $NaOH$ system.

CO_2-aqueous $NaOH$ system satisfies the condition as of equation (4.4.12). Therefore gas phase resistance is negligible. Hence equation (4.4.11) will turn to

$$\frac{1}{K_g} = \frac{H_e}{k_{LR}} \tag{4.4.13}$$

And equation (4.4.10) may be written for calculating interfacial area as follows:

$$a = \frac{G_m{}'He}{k_{LR}P_{CO_2}V_j}\, In\left[\frac{1-y_0}{y_0}\,\frac{y_i}{1-y_i}+\frac{1}{(1-y_i)^3}-\frac{1}{(1-y_0)^3}\right] \qquad (4.4.14)$$

True gas side mass transfer coefficient for chlorine

For Cl_2 aqueous $NaOH$ system

$$k_g p_A \leq \frac{k_{BL}C_{B0}}{z} \qquad (4.4.15)$$

Table 4.4.1 : Typical range of experimental values

Interfacial area	CO_2 aqueous $NaOH$ solution	Cl_2 aqueous $NaOH$ solution	Condition required for
$C_{OH}^0\ kmol/m^3$	0.525	0.525	
$k_2\ kmol/m^3\ s$ at $300K$	9.63×10^3 (Hikita, 1976)	1.7×10^9 (Eq.4.2.37)	
$He\ atm.m^3/kmol$ (Table A3.4)	32 (Patel, 2004)	19.55 (Ashour, 1996)	
$k_g\ kmol/m^3\ atm\ s$	.00037	.00037	
D_g at $303\ K\ m^2/sec$ (Table A3.4)	2.05×10^{-9}	1.68×10^{-9}	
D_{NaOH} at $303K\ m^2/sec$	3.89×10^{-9}	3.89×10^{-9}	
C_g^* at $303K$ in water $kmol/m^3$ (Calculated from Table A3.4)	1.88×10^{-3}	1.39×10^{-3}	
$k_{LR} = [D_{gl}k_2C_{OH}^0]^{1/2}\ m/s$	0.0032	1.22	
$k_{LA}\ m/sec$ apx avg (Radhakrishnan, 1984) and calculated	3.2×10^{-4}	0.009515	
$k_{LB} = k_{LA}(D_B/D_A)\ m/sec$	6.072×10^{-4}	0.022×10^{-4}	
k_{LR}/k_L (eq. no. 4.4.4)	$10 > 3$	$121 > 3$	Fast reaction
$C_{OH}^0/2C_g^*$ (eq. no. 4.4.5)	139 $k_{LR}/k_L \ll C_{OH}^0/2C_g^*$	188 $k_{LR}/k_L \ll C_{OH}^0/2C_g^*$	Pseudo first order
$k_g.He$ (eq. no. 4.4.12)	0.01184 $\therefore k_g.He > k_{LR}$	7.2×10^{-3} $\therefore k_g.He \not> k_{LR}$	Gas phase resistance negligible
$k_g.p_A$	–	1.09×10^{-5}	
$k_{LB}.C_{B0}/z$ (eq. no. 4.4.15)	–	5.78×10^{-3} $\therefore k_G.p_A \leq k_{LB}.C_{B0}/z$	Gas resistance control

That implies that gas phase resistance controls the rate of reaction (Levenspiel, 1999).

Therefore the rate of absorption of Cl_2 may be written as

$$R_{Cl_2}.a = k_G.a.p_A^* \tag{4.4.16}$$

$$k_G.a = \frac{R_{Cl_2}.a}{p_A^*} \tag{4.416a}$$

The true gas side mass transfer coefficient, k_G, is given by,

$$k_G = \frac{k_G a}{a} \tag{4.4.17}$$

The model presented by the equations (4.4.10), (4.4.14) and (4.4.17) are the models to predict the value of a, k_G and $k_G a$.

4.4.3 New mathematical model related to interfacial area for multi nozzle ejectors

Radhakrishnan et al. (1986) have suggested the following correlations to estimates interfacial area i.e.

$$a_{sy} = 225{\chi_1}^{-2.649} \text{ where } \chi_1 \text{ is liquid holdup} \tag{4.4.18}$$

Mandal et al. (2003) have suggested the following estimates for interfacial area of system i.e.

$a = 0.38 \times 10^4 \times v_{gs}$, where v_{gs} is gas superficial velocity

In this work a new model has been proposed for estimation of 'a'. This model is easy to apply and require minimum input data.

r_A is determined experimentally and is equal to $R_A a$.

R_A can be estimated by the model developed in section 4.1 given by expression (4.1.32). So a can be determined

$$R_A a = -r_A \tag{4.4.19}$$

or

$$a = \frac{R_A a}{R_A} \tag{4.4.20}$$

This mathematical model is employed for multi nozzle ejector with number of orifice 3, 5 and 7. The dimensions of multi nozzle ejector are given in chapter 3. The results obtained with this model for multi nozzle ejector are compared with experimental data.

4.4.4 Results and discussions

A new mathematical model has been proposed as per experiment (4.4.16a), (4.4.17) and (4.4.20) to predict mass transfer characteristics by determining the value of $k_G a, k_G$ and a. The predicted values by using this proposed model is presented graphically in the figures (4.4.1) to (4.4.16). The figures show the effect of $C_{Ag,in}$ on predicted value of $k_G a, k_G$ and a for different nozzles and different values of C_{B0}. The values of $R_A a$ is obtained experimentally.

4.4.4.1 Comparison of experimental results of mass transfer characteristics with simulated results

Experimental results and simulated results of mass transfer characteristics, $k_g a, a$ and k_g are plotted together for set up 1 in the figure (4.4.2), (4.4.3) and (4.4.4) respectively. The experimental results are based on equation (4.4.16a), (4.4.14) and (4.4.17). The simulated results are based on the equation (4.4.20) and (4.4.18). The experimental and simulated results are in good agreement. So the model proposed is well fitted.

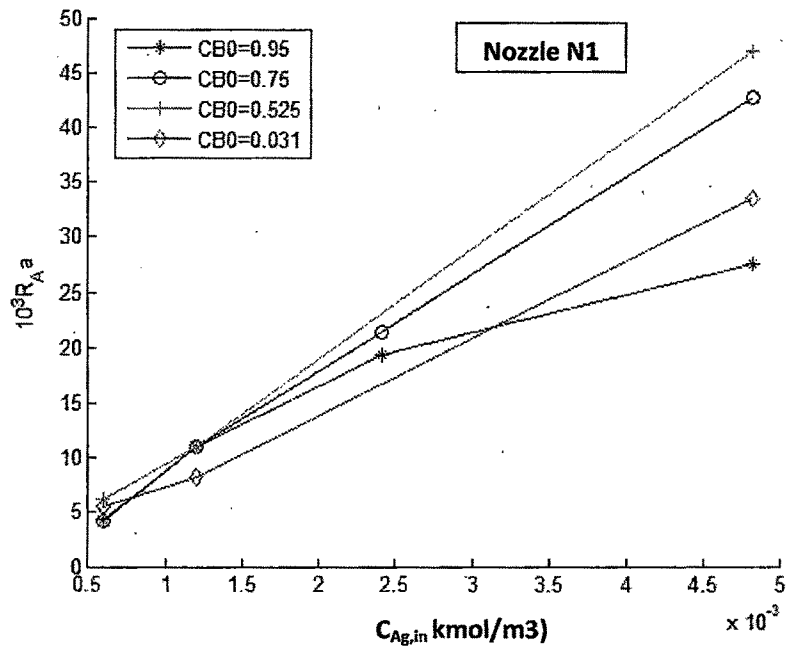

Figure 4.4.1 : Effect of $C_{Ag,in}$ on $R_A a$ for different C_{B0} for setup – 1 with nozzle N1 (no. of orifice 1) (comparison of experimental results and present model)

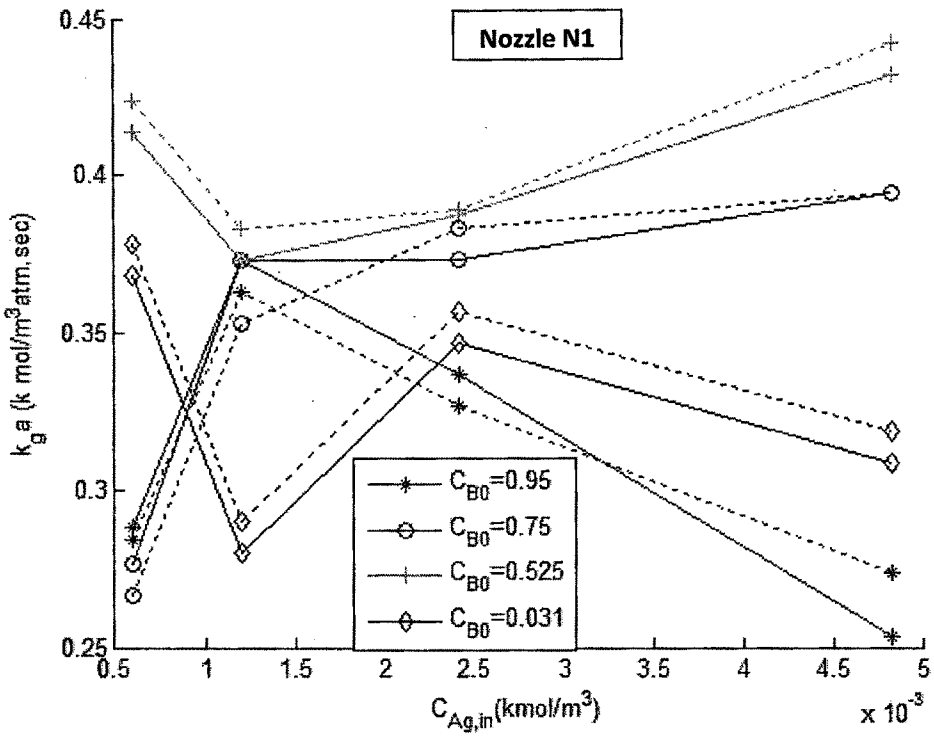

Figure 4.4.2 : Effect of $C_{Ag,in}$ on $k_g a$ for different C_{B0} for setup – 1 with nozzle N1 (no. of orifice 1) (comparison of experimental results and present model)

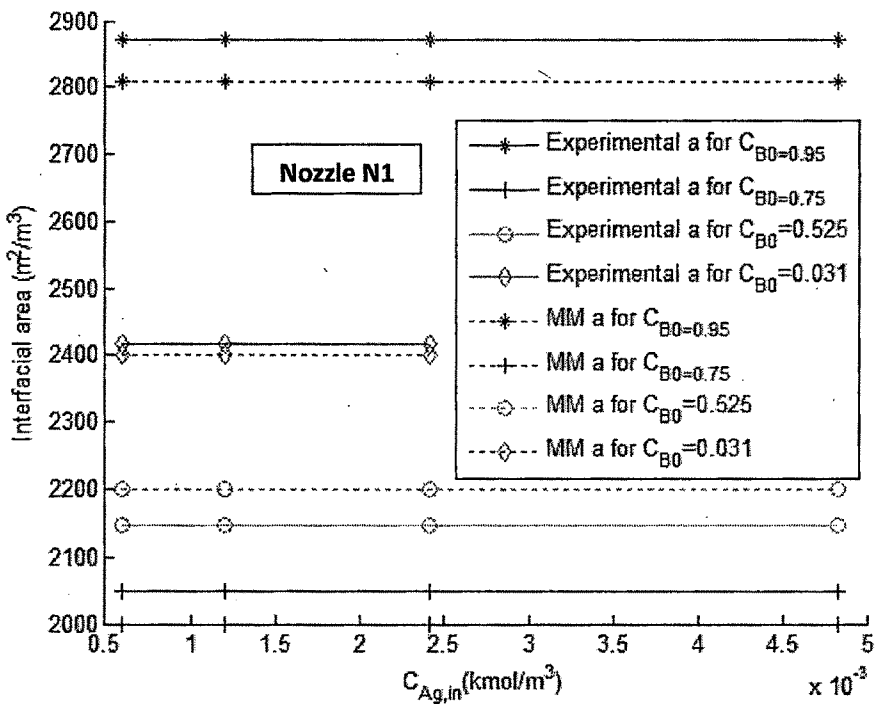

Figure 4.4.3 : Effect of $C_{Ag,in}$ on interfacial area generated in jet ejector for different C_{B0} for setup – 1 with nozzle N 1 (no. of orifice 1) (comparison of experimental results and present model)

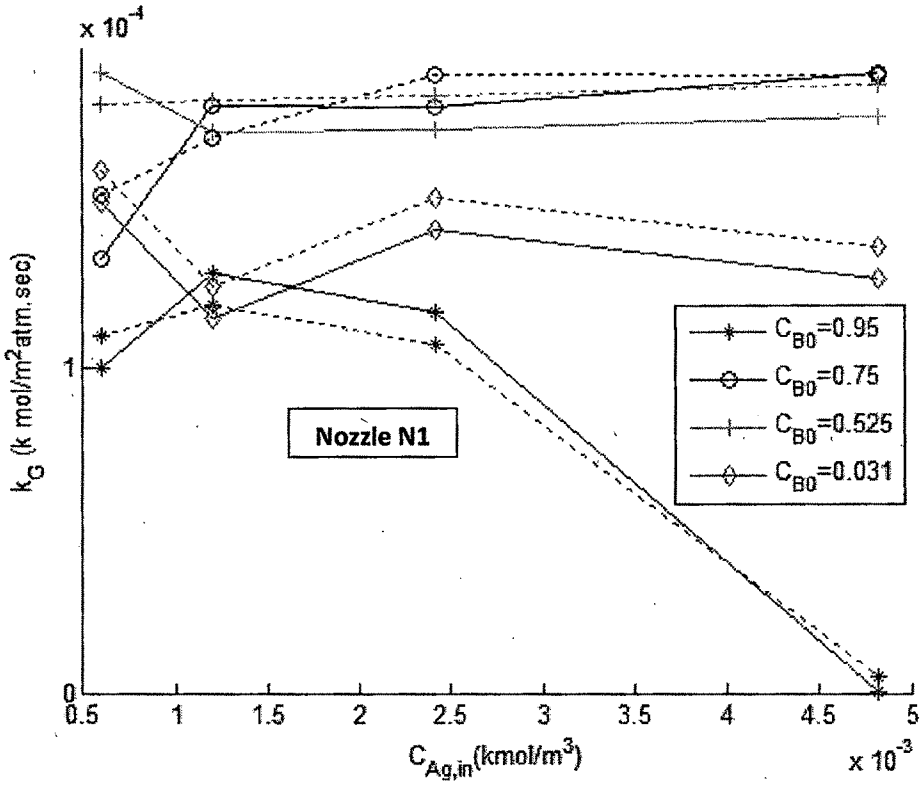

Figure 4.4.4 : Effect of $C_{Ag,in}$ on k_g for different C_{B0} for setup – 1 with nozzle N1 (no. of orifice 1) (comparison of experimental results and present model)

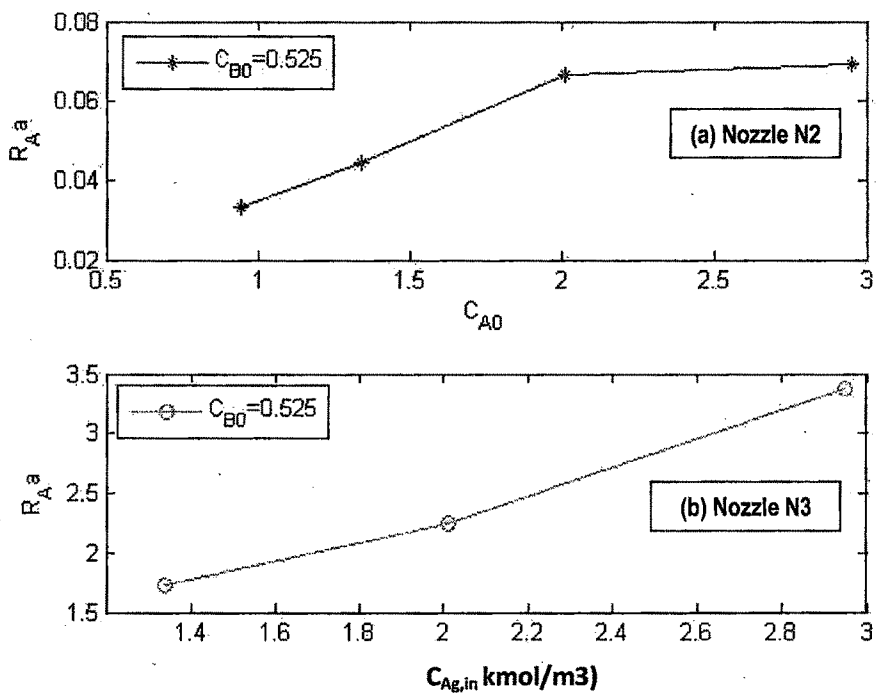

Figure 4.4.5 : Effect of $C_{Ag,in}$ on $R_A a$ for $C_{B0} = 0.525$ for set up 2. (a) with nozzle N2 (no. of orifice 1), (b) with nozzle N3 (no. of orifice 3)

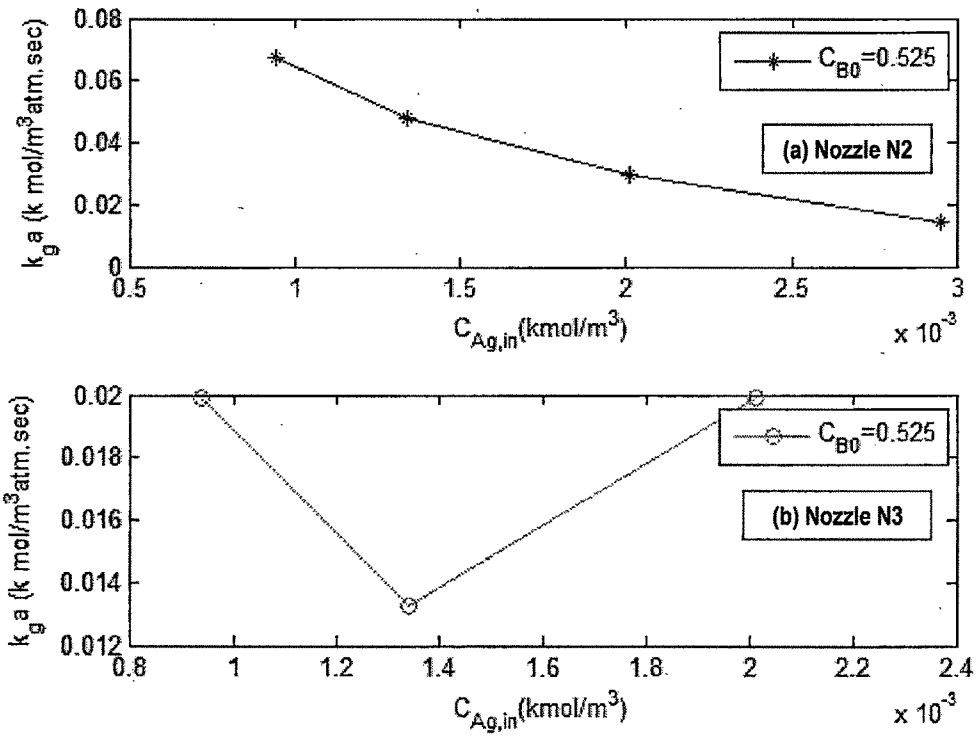

Figure 4.4.6 : Effect of $C_{Ag,in}$ on $k_g a$ for $C_{B0} = 0.525$ for set up 2. (a) with nozzle N2 (no. of orifice 1), (b) with nozzle N3 (no. of orifice 3)

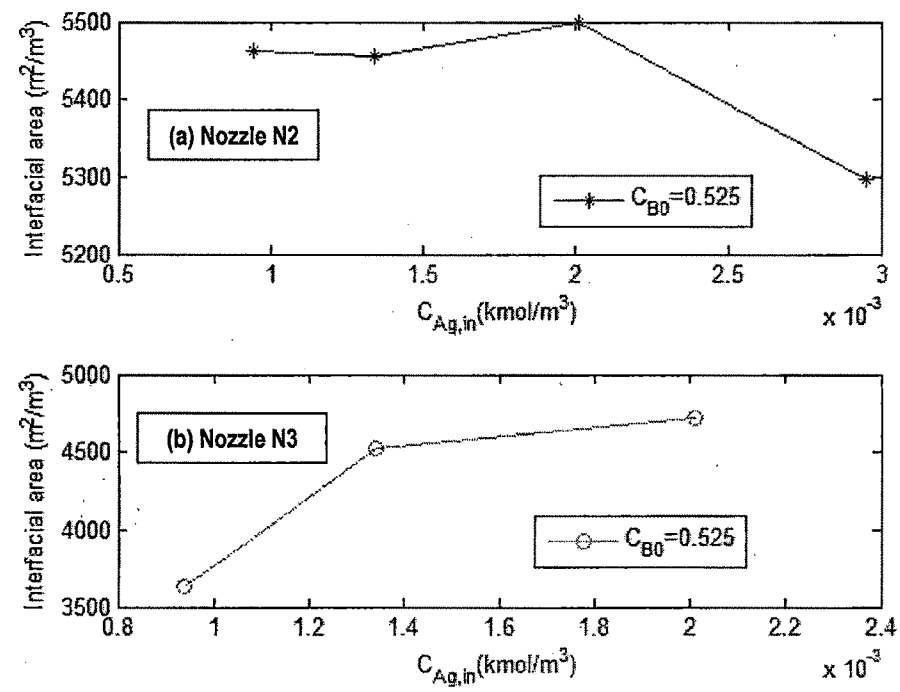

Figure 4.4.7 : Effect of $C_{Ag,in}$ on interfacial area for $C_{B0} = 0.525$ for set up 2. (a) with nozzle N2 (no. of orifice 1), (b) with nozzle N3 (no. of orifice 3)

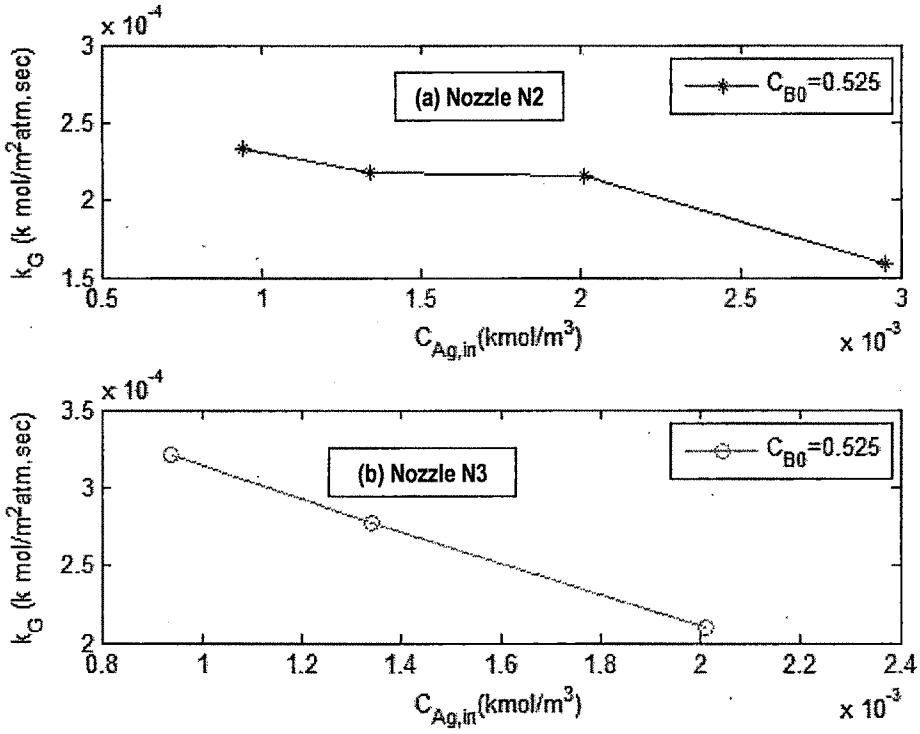

Figure 4.4.8 : Effect of $C_{Ag,in}$ on k_g for $C_{B0} = 0.525$ for set up 2. (a) with nozzle N2 (no. of orifice 1), (b) with nozzle N3 (no. of orifice 3)

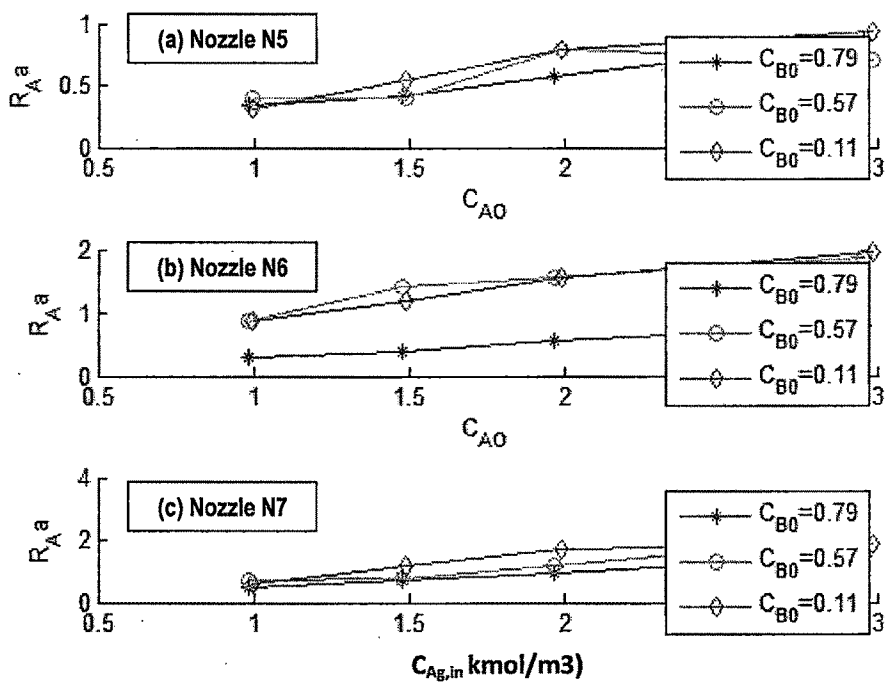

Figure 4.4.9: Effect of $C_{Ag,in}$ on $R_A a$ for different C_{B0} for set up 3. (a) with nozzle N5 (no. of orifice 1), (b) with nozzle N6, (no. of orifice 3), (c) with nozzle N7 (no. of orifice 5)

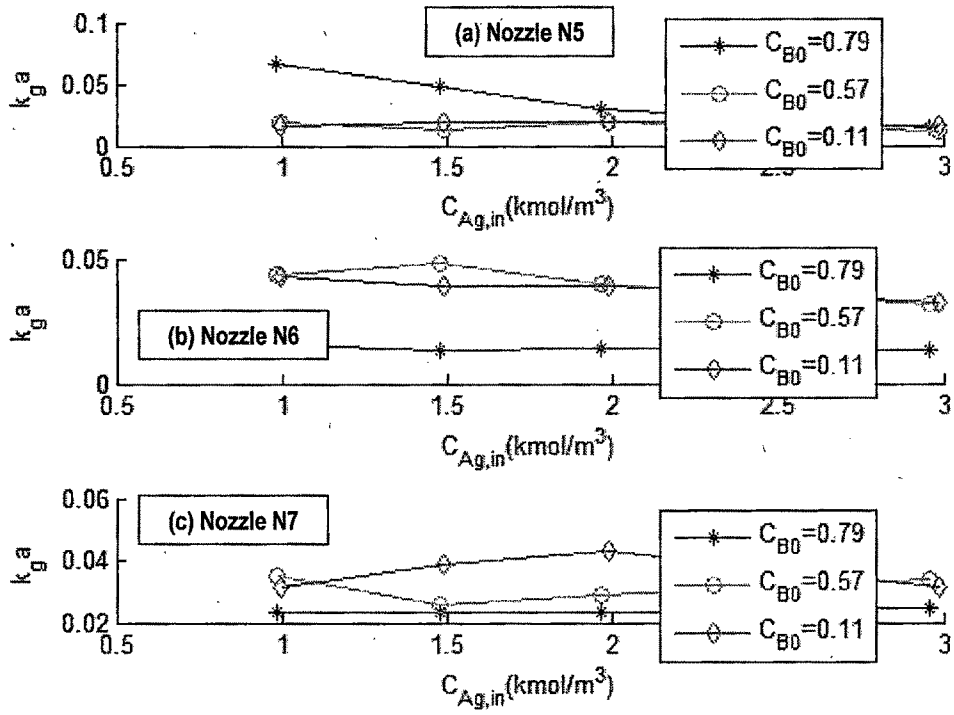

Figure 4.4.10 : Effect of $C_{Ag,in}$ on $k_g a$ for different C_{B0} for set up 3. (a) with nozzle N5 (no. of orifice 1), (b) with nozzle N6, (no. of orifice 3), (c) with nozzle N7 (no. of orifice 5)

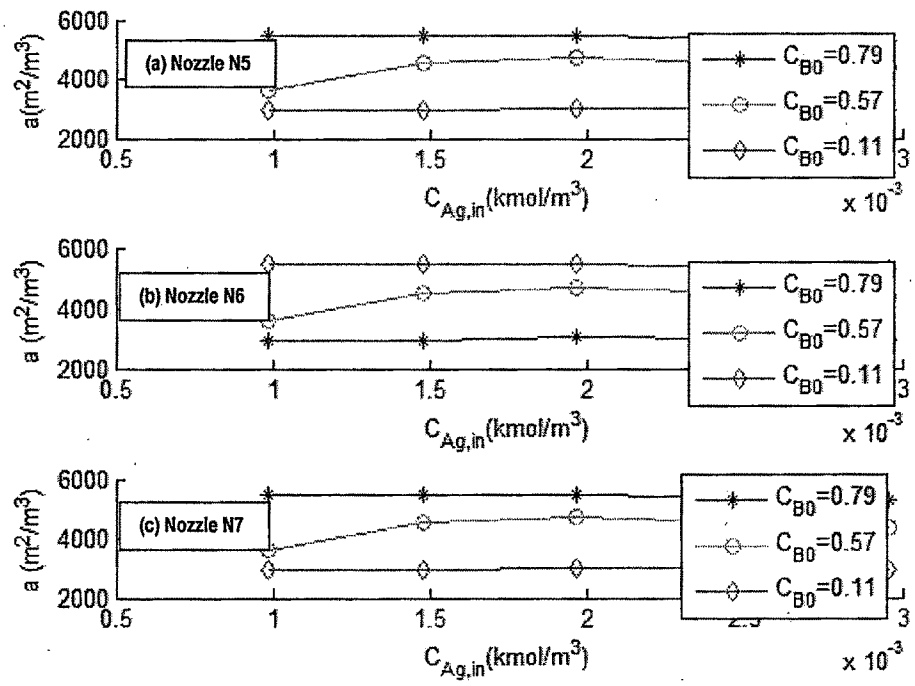

Figure 4.4.11 : Effect of $C_{Ag,in}$ on interfacial area for different C_{B0} for set up 3. (a) with nozzle N5 (no. of orifice 1), (b) with nozzle N6, (no. of orifice 3), (c) with nozzle N7 (no. of orifice 5)

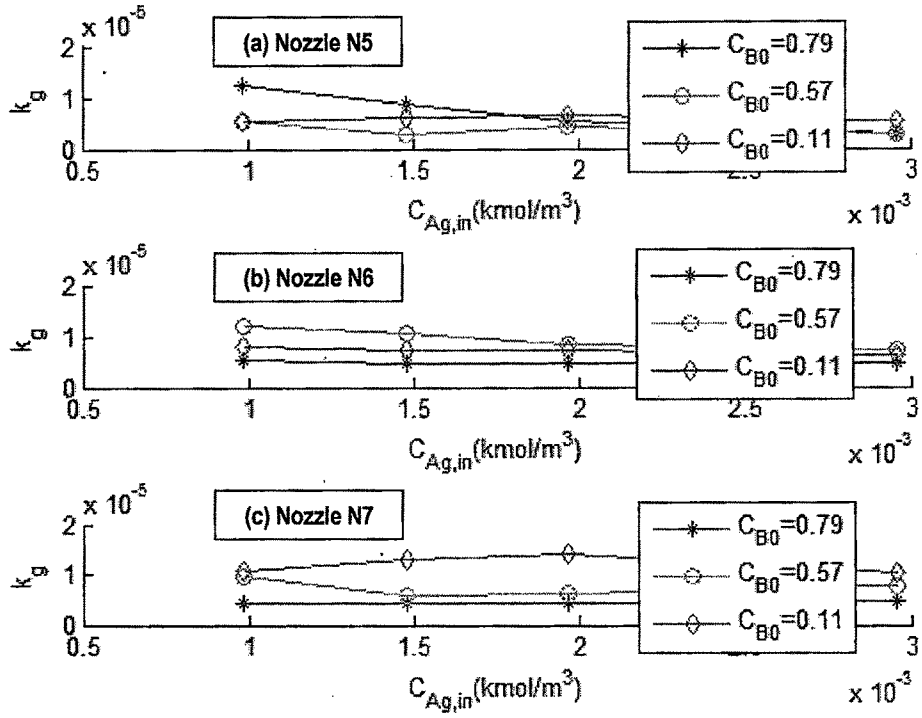

Figure 4.4.12 : Effect of $C_{Ag,in}$ on k_g for different C_{B0} for set up 3. (a) with nozzle N5 (no. of orifice 1), (b) with nozzle N6, (no. of orifice 3), (c) with nozzle N7 (no. of orifice 5)

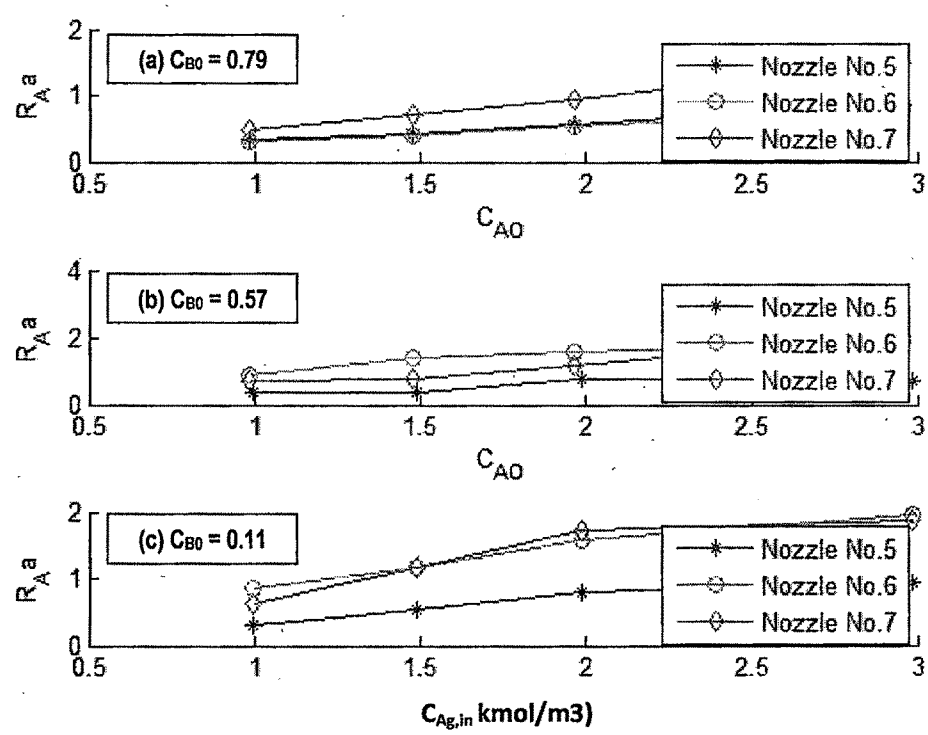

Figure 4.4.13 : Effect of $C_{Ag,in}$ on $R_A a$ for different nozzle for set up 3. (a) with $C_{B0} = 0.79$ (b) with $C_{B0} = 0.57$ (c) with $C_{B0} = 0.11$

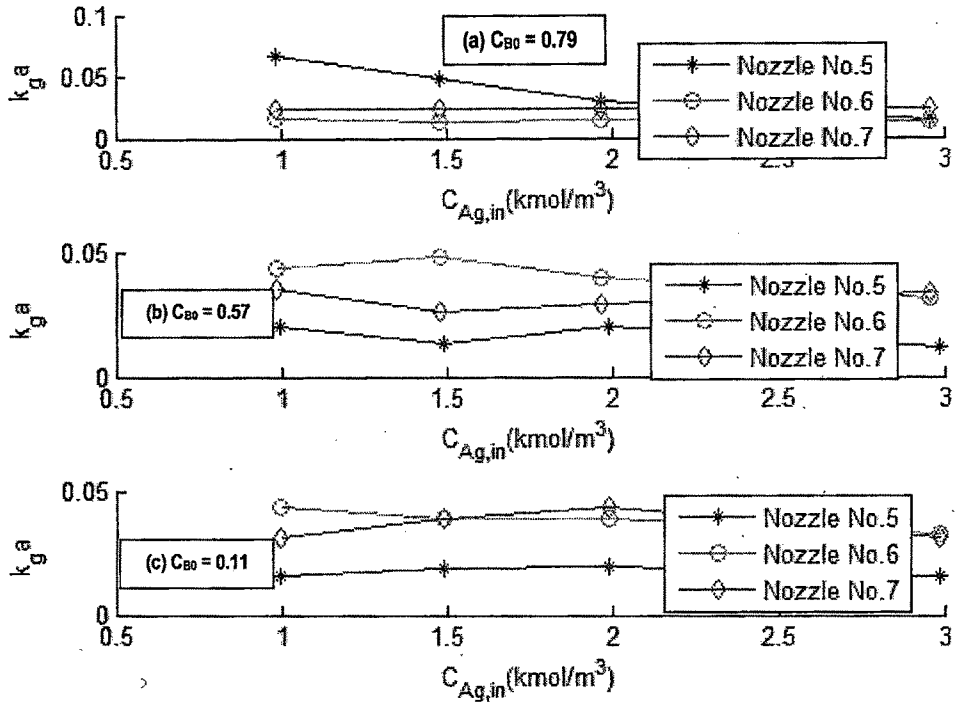

Figure 4.4.14 : Effect of $C_{Ag,in}$ on $k_g a$ for different nozzle for set up 3.
(a) with $C_{B0} = 0.79$ (b) with $C_{B0} = 0.57$ (c) with $C_{B0} = 0.11$

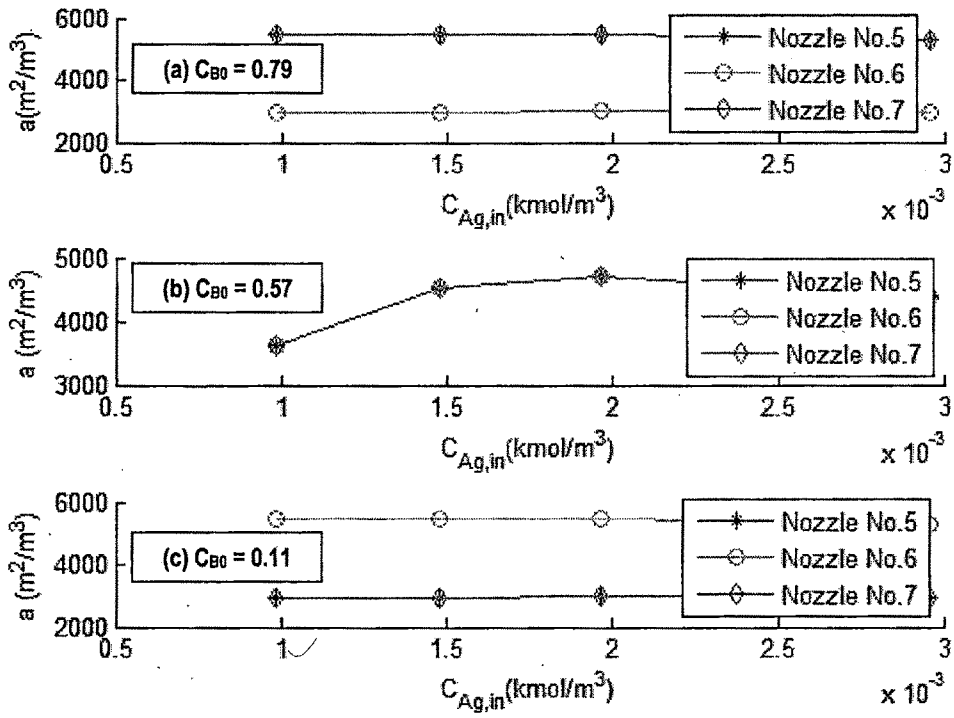

Figure 4.4.15 : Effect of $C_{Ag,in}$ on interfacial area for different nozzle for set up 3.
(a) with $C_{B0} = 0.79$ (b) with $C_{B0} = 0.57$ (c) with $C_{B0} = 0.11$

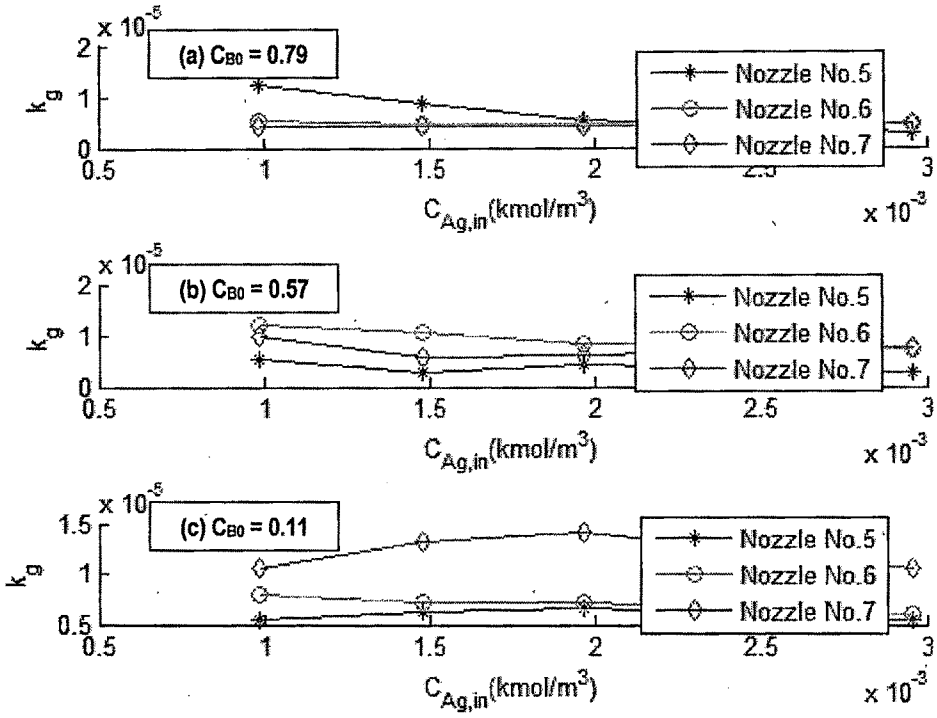

Figure 4.4.16 : Effect of $C_{Ag,in}$ on k_g for different nozzle for set up 3.
(a) with $C_{B0} = 0.79$ (b) with $C_{B0} = 0.57$ (c) with $C_{B0} = 0.11$

4.4.4.1 Factors affecting rate of absorption ($R_A a$) in liquid jet ejector

Figure (4.4.1), (4.4.5), (4.4.9) and (4.4.13) show the effect of $C_{Ag,in}$ on $R_A a$ using different nozzles. The following conclusions can be derived from the study of the figures.

- A common trend has emerged that as $C_{Ag,in}$ increases the $R_A a$ also increases in all setups for all nozzles. This is because rate of reaction is function of concentration of both reactants i.e. chlorine ($C_{Ag,in}$) and $NaOH$ (C_{B0}).

- As C_{B0} increases the $R_A a$ decreases.The concentration of aqueous $NaOH$ solution in C_{B0} is kept high to maintain pseudo first order condition i.e. rate of reaction is independent of concentration of C_{B0}. The reduction in rate of absorption is due to (1) the increase in viscosity of aqueous $NaOH$ solution (2) reduction of physical solubility of Cl_2 (Krevelen and Hoftijzer theory, 1948).and (3) decrease in diffusivity coefficient (Stokes-Einstein equation) when concentration of $NaOH$ increases.

- $R_A a$ is higher for higher number of nozzles (figure-4.4.13). This is because the exposed outer surface of liquid jet in the free jet section is higher for more number of nozzles having same flow area. The high liquid jet exposed outer surface counters the

effect of increase in viscosity of aqueous $NaOH$ solution due to increase in its concentration. But for lower concentration of C_{B0}, the value of $R_A a$ is maximum for nozzle N6 (three nozzle). The value of $R_A a$ is minimum for nozzle N5 (single nozzle).

- The maximum absorption obtained is in vertical installation in setup 3 having nozzle N6 (no. of orifice 3).

4.4.4.3 Effect of different parameters on mass transfer characteristics ($k_g a$, a and k_g) in jet ejectors

Effect of C_{B0} on $k_g a$, a and k_g

Volumetric mass transfer coefficient ($k_g a$) predicted by proposed model versus $C_{Ag,in}$ for setup 1, 2 and 3 are shown in figure (4.4.2), (4.4.6), (4.4.10) and (4.4.14).

Interfacial area (a) predicted by proposed model versus $C_{Ag,in}$ for setup 1, 2 and 3 are presented in figure (4.4.3), (4.4.7) and (4.4.11).

True gas side mass transfer coefficient (k_g) predicted by proposed model versus $C_{Ag,in}$ for setup 1, 2 and 3 are presented in figure (4.4.4), (4.4.12) and (4.4.16).

The figures shows that the interfacial area first decreases with increase in C_{B0} then it rises with increase in C_{B0}. The increase in C_{B0} have two phenomenon simultaneously: (1) the viscosity increases (2) electrolyte concentration increases. By increasing viscosity the diffusivity and solubility of gas both decreases which have negative effect on absorption. While increase in electrolytes leads to a strong hindrance on bubble coalescence. This will lead to major decrease of the mean bubble size. Therefore interfacial area and the volumetric mass transfer coefficient both increases. (Bailer, 2001; Havelka et al., 2000; Kordac and Linek, 2008). Thus depending upon the influence of these parameters, there is net rise or fall in $k_g a$ and k_g. In most of cases the value of $k_g a$ and k_g are lower at higher C_{B0}.

Effect of number of nozzles on $k_g a$, a and k_g

The effect of number of nozzle on volumetric mass transfer coefficient $k_g a$ predicted by proposed model with respect to $C_{Ag,in}$ at different C_{B0} are shown in figure (4.4.6) and (4.4.14). The figure (4.4.6) is a plot of the $k_g a$ vs $C_{Ag,in}$ for setup 2 at C_{B0} = 0.527 for nozzle N2 (having number of orifice 1) and N3 (having number of orifice 3). The

figure (4.4.14) is a plot of the $k_g a$ vs $C_{Ag,in}$ for setup 3 at different C_{B0} for nozzle N5 (having number of orifice 1), N6 (having number of orifice 3) and N7 (having number of orifice 5).

The effect of number of nozzle (orifice) on interfacial area 'a' generated are shown in the figure (4.4.7) and (4.4.15).

True gas side mass transfer coefficient (k_g) is studied in the figure (4.4.8) and (4.4.16) for different nozzles (N2, N3, N5, N6 and N7) at different C_{B0}.

It is observed that at lower C_{B0} the $k_g a$ and k_g are higher for nozzle N7 (no. of orifice 5) and at higher C_{B0} the $k_g a$ and k_g are higher for nozzle N5 (no. of orifice 1). Similar effect is observed for setup 2 (figure 4.4.6 and 4.4.8) where the $k_g a$ is higher for nozzle N2 (no. of orifice 1) compared to nozzle N3 (no. of orifice 3).

As numbers of nozzle (orifice) are increased the outer exposed area of free jet is more for same flow area. The higher outer exposed area makes entrainment of gas easy to the free jet. The higher C_{B0} also lead to increase in viscosity, which resist gas to enter in the liquid stream. So at higher C_{B0} the effect of higher outer exposed area is compensated and we are getting lower value of k_g and $k_g a$ for higher number of orifice.

It is also observed that at high C_{B0} (0.79 kmol/m^3) the higher interfacial area is obtained for nozzle N5 and N7 (no. of orifice 1 and 5 respectively). For intermediate C_{B0} (0.57 kmol/m^3 for setup 3 and 0.52 kmol/m^3 for setup 2) the interfacial area is almost same for all nozzle. While for lower C_{B0} (0.11 kmol/m^3) the interfacial area is more for nozzle 6 (no. of orifice 3). As number of orifice (nozzle) increases there is collision of jet at the entry of throat which has negative effect on the interfacial area. Thus the effect of more outer exposed area and collision of jet enhances the interfacial area for number of more nozzles.

Effect of $C_{Ag,in}$ on $k_g a$, a and k_g

The variation $k_g a, a$ and k_g with respect to $C_{Ag,in}$ is shown in figures (4.4.1) to (4.4.16).

- **Volumetric mass transfer coefficient ($k_g a$):** The effect of $C_{Ag,in}$ on $k_g a$ by variation in C_{B0} and no. of nozzle are shown in figures (4.4.2), (4.4.6), (4.4.10) and (4.4.14). All the figures are almost similar qualitatively i.e. as the value of $C_{Ag,in}$

increases the value of $k_g a$ decreases. The decrease is very sharp at initial values of $C_{Ag,in}$. Afterwards the decrease in $k_L a$ with respect to $C_{Ag,in}$ is reduced.

- **Mass transfer coefficient (k_g):** The effect of $C_{Ag,in}$ on k_g is shown in figures (4.4.4), (4.4.8), (4.4.12) and (4.4.16). Form figures it is seen that there is decrease in he value of k_g with respect to $C_{Ag,in}$ except some exception.

The trend of decrease in $k_g a$ and k_g is because of effect of reactant ratio C_{B0}/C_A^* on reaction factor. As discussed in section (4.2); the increase of reaction ratio C_{B0}/C_A^* this will lead to increase in enhancement factor. The rate of increase in enhancement factor is sharp at the lower value of C_{B0}/C_A^* ratio and then decreases and become negligible. The C_A^* is the function of $C_{Ag,in}$ as per Henry's law. Therefore as C_{A0} increases the enhancement factor also decreases. The enhancement factor is direct function of mass transfer coefficient ratio of absorption with and without chemical reaction.

Interfacial area 'a': The effect of $C_{Ag,in}$ on interfacial area for different nozzles and at different C_{B0} is shown in figures (4.4.3), (4.4.7), (4.4.11) and (4.4.15). It is observed that there is only a little variation in interfacial area with change in $C_{Ag,in}$. This is because the interfacial area generated depends on liquid to gas ratio and viscosity of the liquid. In the present experiment the liquid to gas ratio is kept constant and very low concentration of Cl_2 has been used. Under these conditions the viscosities of liquid and gas will not change significantly.

4.4.5 Conclusion

- Correlations for prediction of the liquid holdup in a multi-jet ejector contactor system have been proposed by the equation (4.4.3).
- The model to predict interfacial area is presented by the equation (4.4.14). A new model have also been proposed to predict the interfacial area a by the correlation (4.4.20). For utilizing this correlation the experimental data of the system does not required to satisfy the condition (4.4.12).
- To predict $k_g a$ and k_g a model is presented by the equation (4.4.10) and (4.4.17). These model is compared with the model developed in section (4.1) by equation (4.1.28).

- The figures (4.4.1) to (4.4.16) are plotted on the basis of the prediction from proposed new model presented by equations (4.4.20). The behavior of $k_g a, a$ and k_g are shown against different initial concentration of gases for different nozzles and C_{B0} in these figures. The results are summarized in the following table.

Table 4.4.2 : Summary of analysis of results for different C_{B0} and nozzles

	C_{B0}	$C_{Ag,in}$	Number of nozzle
$R_A a$	decreases	increases	increases
$k_g a$	decreases except N5	decreases	increases except C_{B0}=0.79
a	decreases then increases except N1	≈ constant	constant for C_{B0}=0.57
k_g	decreases except N5	constant except N1 at C_{B0}=0.95	increases except C_{B0}=0.79

4.5 Removal efficiency of chlorine in jet ejector (Chlorine aqueous $NaOH$ solution)

The major factors which affect the efficiency of jet ejector are liquid flow rate, gas flow rate, the concentration of absorbing liquid and the concentration of the solute in the gas.

Ravindram and Pyla (1986) proposed a theoretical model for the absorption of SO_2 and CO_2 in dilute $NaOH$ based on simultaneous diffusion and irreversible chemical reaction for predicting the amount of gaseous pollutant removed.

Many researchers (Volgin et al., 1968; Ravindram and Pyla, 1986; Cramers et al., 1992, 2001; Gamisans et al., 2002; Mandal, 2003, 2004, 2005; Balamurugan et al., 2007, 2008; Utomo et al., 2008; Yadav, 2008; Li and Li, 2011.) have reported different theories and correlations to predict scrubbing efficiency of jet ejectors.

Uchida and Wen (1973) developed a mathematical model to predict the removal efficiency of SO_2 into water and alkali solution. The simulated results of their model were compared with experimental results and they found that there is a good agreement with the experimental results. They have also found enhancement factor to predict rate of the chemical absorption.

Gamisans et al. (2002) evaluated the suitability of an ejector-venturi scrubber for the removal of two common stack gases, sulphur dioxide and ammonia. They studied the influence of several operating variables for different geometries of venturi tube. A statistical approach was presented by them to characterize the performance of scrubber by varying several factors such as gas pollutant concentration, gas flow rate and liquid flow rate. They carried out the computation by multiple regression analysis making use of the method of the least squares method. They have used commercial software package, STATGRAPHICS, to determine the multiple regression coefficients.

Less attention has been paid in the area of mathematical and statistical modeling. The statistical models have edge over other models due to their capacity to handle random data correctly. There are several techniques available to relate the controllable factors and experimental facts.

In this chapter, we have made an attempt to develop statistical model based on non linear quadratic multiple regression analysis to predict removal efficiency of jet ejector for Cl_2-aqueous $NaOH$ system.

4.5.1 Statistical modeling

We have used the non linear quadratic relation between independent variables and dependent variables and is as follows:

$$Y = \Psi_0 + \sum_{i=1}^{n} \Psi_i X_i + \sum_{i=1}^{n} \sum_{j=1}^{n} \Psi_{ij} X_i X_j \qquad (4.5.1)$$

Here, Y is a response variable, X is the main factor; Ψ_0 is the constant value of the regression; Ψ_i is the linear coefficient; Ψ_{ii} is the quadratic coefficient and Ψ_{ij} is the interaction coefficient. When $i = j.$; $\Psi_{ij} = \Psi_{ji}$ and $2\Psi_{ij} = \Psi'_{ij}$.

The computation was carried out by non linear regression analysis making use of the generalized minimal residual method.

The non linear regression coefficients determined by computation with the software package, STATGRAPHICS Plus 4.0, were used to determine the optimal model fitting.

4.5.2 Results and discussions

The factors which affect the absorption efficiency are gas concentration and the scrubbing liquid concentration. In this work the jet ejector is operated on critical value of liquid flow

rate. For a given geometry, reduction in the liquid flow rate will lead to reduction of induced gas flow rate. Therefore, in the present work the liquid flow rate is kept constant. Effect of C_{B0} and $C_{Ag,in}$ on the removal efficiency ($\%RE$) of the ejector have been investigated in this work.

The experimental values for the operating variables used in the present work are presented in Table 4.5.1 and the experimental data are tabulated in Table 4.5.2 and 4.5.3.

Table 4.5.1 : Codification of the operating variables for the statistical analysis

Code	Variable	Values
X_1	Gas concentration (kmole/m^3)	$(0.6\ to\ 4.3) \times 10^{-3}$
X_2	Liquid concentration (kmole/m^3)	$0 - 0.95$
Y	Removal efficiency (%)	0 - 100

Table 4.5.2 : Experimental matrix for chlorine removal efficiency using setup – 1

No.	$10^3 C_{Ag,in}$ $(kmole/m^3)$	$10^3\ C_{B0}$ $(kmole/m^3)$	RE (%)
1	0.605	0.950	10.0
2	1.193	0.950	83.2
3	2.315	0.950	75.1
4	4.386	0.950	56.3
5	0.605	0.750	61.0
6	1.193	0.750	82.4
7	2.315	0.750	82.28
8	4.386	0.750	86.86
9	0.605	0.525	91.40
10	1.193	0.525	82.41
11	2.315	0.525	21.23
12	4.386	0.525	95.27
13	0.605	0.310	81.25
14	1.193	0.310	61.80
15	2.315	0.310	74.32
16	4.386	0.310	68.09
17	0.605	0.0	41.00
18	1.193	0.0	41.20
19	2.315	0.0	42.50
20	4.386	0.0	25.21

Table 4.5.3 : Experimental matrix for chlorine removal efficiency using setup – 3

Run No.	Nozzle No.	$10^3 C_{Ag,in}$ $(kmole/m^3)$	$10^3\ C_{B0}$ $(kmole/m^3)$	RE (%)
301	N5	2.95538	0.79	21.07
302		1.966803	0.79	43.18
303		1.475102	0.79	69.09
304		0.983402	0.79	97.88
321	N5	2.984934	0.57	47.42
322		1.986471	0.57	57.01
323		1.489853	0.57	57.01
324		0.993236	0.57	62.71
325	N5	2.984934	0.11	36.04
326		1.986471	0.11	34.20
327		1.489853	0.11	34.20
328		0.993236	0.11	34.20
305	N6	2.95538	0.79	17.24
306		1.966803	0.79	28.79
307		1.475102	0.79	19.19
308		0.983402	0.79	28.79
317	N6	2.95538	0.57	45.98
318		1.966803	0.57	57.58
319		1.475102	0.57	69.09
320		0.983402	0.57	63.33
329	N6	2.984934	0.11	49.32
330		1.986471	0.11	42.75
331		1.489853	0.11	38.00
332		0.993236	0.11	51.31
309	N7	2.95538	0.79	22.99
310		1.966803	0.79	28.79
311		1.475102	0.79	26.87
312		0.983402	0.79	23.03
313	N7	2.95538	0.57	19.16
314		1.966803	0.57	20.15
315		1.475102	0.57	19.19
316		0.983402	0.57	23.03
333	N7	2.984934	0.11	45.53
334		1.986471	0.11	62.71
335		1.489853	0.11	57.01
336		0.993236	0.11	45.61

4.5.2.1 Statistical analysis

STATGRAPHICS Plus 4.0 is used to predict the removal efficiency (Y) using statistical model (4.5.1) for the nozzles N1, N5, N6 and N7.The results are summarized in table (4.5.4) and (4.5.5) Table (4.5.4) demonstrates the parameters as outcome of simulated results of STATGRAPHICS plus 4.0. The regression coefficients of fitted models are summarized in table (4.5.5).

The analysis of variance (ANOVA) for the operational variables C_{B0} and $C_{Ag,in}$ indicate that removal efficiency is well described by nonlinear quadratic models. The convergence is obtained successfully after 4 iterations for estimation of regression coefficients.

Furthermore, the statistical analysis showed that both factors (C_{B0} and $C_{Ag,in}$) had significant effects on the response (RE) and the liquid concentration is more significant between two.

It may be observed that fitted models do not contain the independent term (Ψ_0). This implies that the removal efficiency (RE) is a function of the factors considered only.

Table 4.5.4 : Parameters for multiple regression analysis

Properties to be Operated	Nozzle N1 for Setup – 1 with no. of orifice 1	Nozzle N5 for Setup – 3 with no. of orifice 1	Nozzle N6 for Setup – 3 with no. of orifice 3	Nozzle N7 for Setup – 3 with no. of orifice 5
Adopted Technique	Nonlinear Regression	Nonlinear Regression	Nonlinear Regression	Nonlinear Regression
Dependent variable	Y	Y	Y	Y
Independent variables	X_1, X_2	X_1, X_2	X_1, X_2	X_1, X_2
Function to be estimated	b_1X_1 $+b_2X_2$ $b_{11}X_1X_1$ $+ b_{22}X_2X_2$ $+ b_{12}X_1X_2$	b_1X_1 $+b_2X_2$ $b_{11}X_1X_1$ $+ b_{22}X_2X_2$ $+ b_{12}X_1X_2$	b_1X_1 $+b_2X_2$ $b_{11}X_1X_1$ $+ b_{22}X_2X_2$ $+ b_{12}X_1X_2$	b_1X_1 $+b_2X_2$ $b_{11}X_1X_1$ $+ b_{22}X_2X_2$ $+ b_{12}X_1X_2$
Initial parameter estimates	b_1=0.1 b_2=0.1 b_{11}=0.1 b_{22}=0.1 b_{12}=0.1	b_1=0.1 b_2=0.1 b_{11}=0.1 b_{22}=0.1 b_{12}=0.1	b_1=0.1 b_2=0.1 b_{11}=0.1 b_{22}=0.1 b_{12}=0.1	b_1=0.1 b_2=0.1 b_{11}=0.1 b_{22}=0.1 b_{12}=0.1
Estimation method	Marquardt	Marquardt	Marquardt	Marquardt

Table 4.5.4 continued

Continued from previous page

	Estimation stopped due to convergence of residual sum of squares.	Estimation stopped due to convergence of residual sum of squares.	Estimation stopped due to convergence of residual sum of squares.	Estimation stopped due to convergence of parameter estimates.
Number of iterations	4	4	4	4
Number of function calls	26	26	26	25
Fitted model	$Y = 11.1059X_1 + 205.385X_2 + 0.688086X_1X_1 \pm 72.5912X_2X_2 \pm 56.7127X_1X_2$	$Y = 20.6505X_1 + 263.417X_2 - 4.09009X_1X_1 \pm 293.901X_2X_2 \pm 16.134X_1X_2$	$Y = 67.9698X_1 - 99.2834X_2 - 15.4581X_1X_1 + 95.9406X_2X_2 \pm 17.0609X_1X_2$	$Y = 17.4129X_1 + 166.782X_2 - 0.923805X_1X_1 \pm 88.6827X_2X_2 \pm 19.0502X_1X_2$

Table 4.5.5 : Regression coefficient from multi regression analysis

Parameters	Nozzle N1 for Setup – 1 with no. of orifice 1	Nozzle N5 for Setup – 3 with no. of orifice 1	Nozzle N6 for Setup – 3 with no. of orifice 3	Nozzle N7 for Setup – 3 with no. of orifice 5
b_1	11.1059	20.6505	67.9698	17.4129
b_2	205.385	263.417	- 99.2834	166.782
b_{11}	0.688086	- 4.09009	- 15.4581	- 0.923805
b_{22}	± 72.5912	± 293.901	+ 95.9406	± 88.6827
b_{12}	± 56.7127	± 16.134	± 17.0609	± 19.0502

Tests are run to determine the goodness of fit of a model and how well the non linear regression plot approximates the experimental data. As the results are multi numerical they are presented in figures (4.5.1) to (4.5.20) and tables (4.5.A-1) to (4.5.D-4). Statistical tests like R-squared, R-squared (adjusted for d.f.), standard error of estimate, mean absolute error and Durbin-Watson statistic are covered. The tables containing confidence interval, analysis of variance (ANOVA) and residual analysis are also reported.

4.5.2.2 Results of statistical analysis in STATGRAPHICS Plus 4 for different nozzles:

Nozzle N1 for Setup – 1 with no. of orifice 1

Table 4.5.A-1 : Estimation Results for nozzle N1

Parameter	Estimate	Asymptotic Standard Error	Asymptotic 95.0% Confidence Interval	
			Lower	Upper
b1	11.1059	10.7826	-14.391	36.6028
b2	205.385	53.6661	78.4841	332.285
b11	0.688086	3.79419	-8.28378	9.65995
b22	-72.5912	58.9481	-211.982	66.7993
b12	-56.7127	12.1159	-85.3623	-28.0631

Table 4.5.A-2 : Analysis of Variance for nozzle N1

Source	Sum of Squares	Df	Mean Square
Model	33479.5	5	6695.9
Residual	672.16	7	96.0228
Total	34151.7	12	
Total (Corr.)	4747.67	11	

Table 4.5.A-3 : Results of statistical tests for nozzle N1

Estimation	Validation
N	12
MSE	96.0228
MAE	6.18318
MAPE	12.8496
ME	0.257439
MPE	-0.445066

Table 4.5.A-4 : Residual Analysis for nozzle N1

R-Squared	85.8423 %
R-Squared (adjusted for d.f.)	77.7522 %
Standard Error of Estimate	9.79912
Mean absolute error	6.18318
Durbin-Watson statistic	0.891519

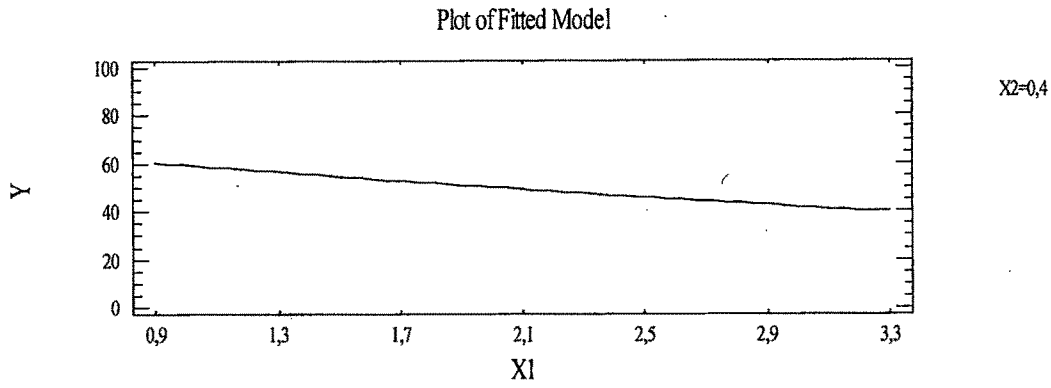

Figure 4.5.1: Removal efficiency (Y) versus gas concentration (X_1) for constant liquid concentration ($X_2 = 0.4$) for nozzle N1

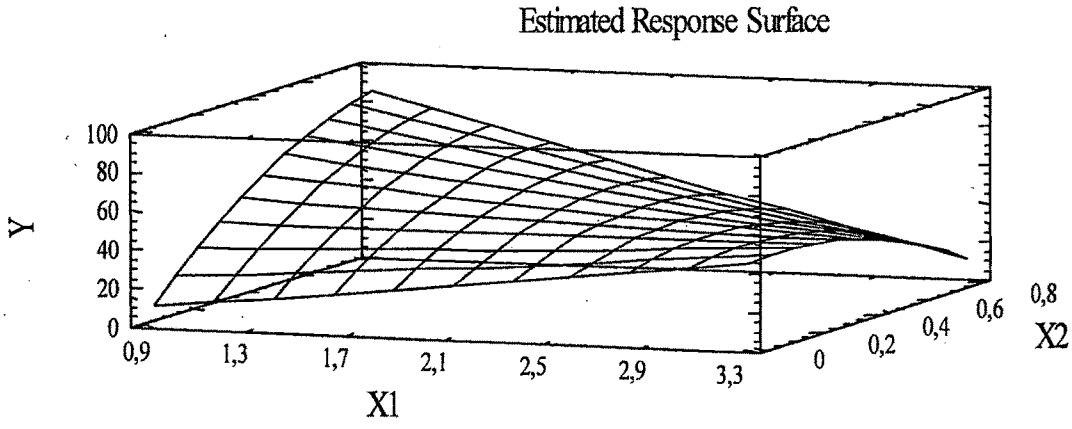

Figure 4.5.2 : Removal efficiency (Y) response surface versus gas concentration (X_1) and liquid concentration (X_2) for nozzle N1

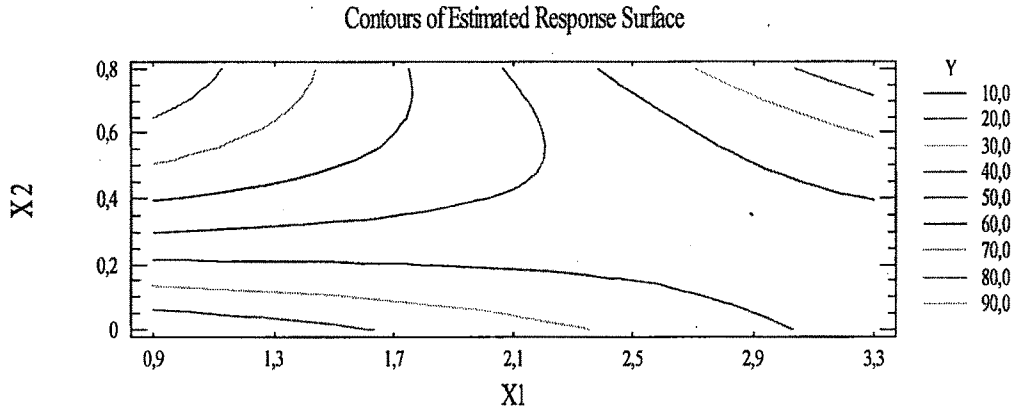

Figure 4.5.3 : Contour plot for Removal efficiency (Y) for nozzle N1

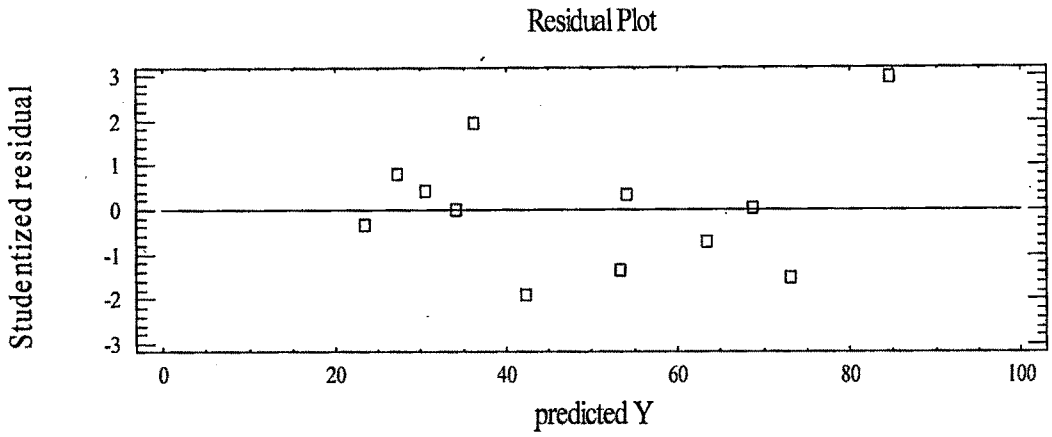

Figure 4.5.4 :Predicted removal efficiency (Y) versus observed removal efficiency (Y) for nozzle N1

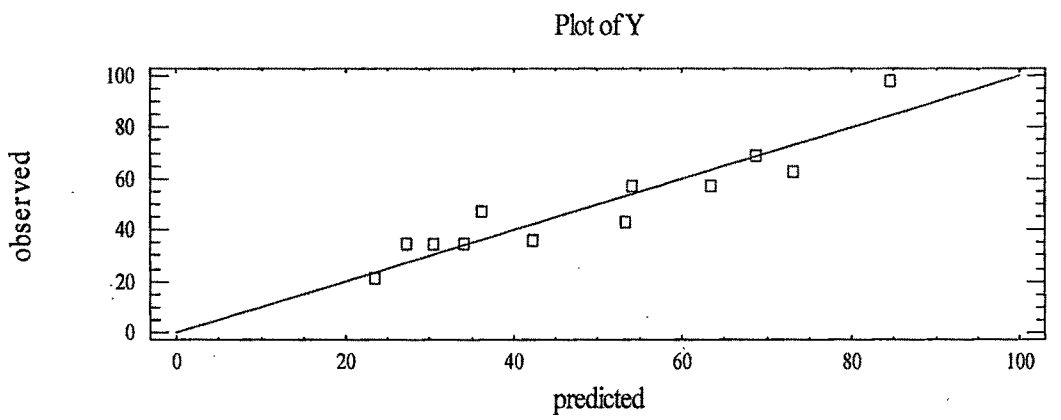

Figure 4.5.5 :Residual Plot for nozzle N1

Nozzle N5 for Setup – 3 with no. of orifice 1

Table 4.5.B-1 : Estimation Results for nozzle N5

Parameter	Estimate	Asymptotic Standard Error	Asymptotic 95.0% Confidence Interval	
			Lower	Upper
b1	20.6505	8.51199	0.522786	40.7782
b2	263.417	42.0993	163.868	362.966
b11	- 4.09009	2.9974	-11.1778	2.99764
b22	- 293.901	46.3188	-403.427	-184.374
b12	- 16.134	9.4982	-38.5937	6.32578

Table 4.5.B-2 : Analysis of Variance for nozzle N5

Source	Sum of Squares	Df	Mean Square
Model	24459.2	5	4891.85
Residual	414.451	7	59.2073
Total	24873.7	12	
Total (Corr.)	3082.07	11	

Table 4.5.B-3 : Results of statistical tests for nozzle N5

R-Squared	86.5528 %
R-Squared (adjusted for d.f.)	78.8687 %
Standard Error of Est.	7.69463
Mean absolute error	5.15937
Durbin-Watson statistic	1.95717

Table 4.5.B-4 : Residual Analysis for nozzle N5

Estimation	Validation
N	12
MSE	59.2073
MAE	5.15937
MAPE	14.7485
ME	0.271349
MPE	-0.381023

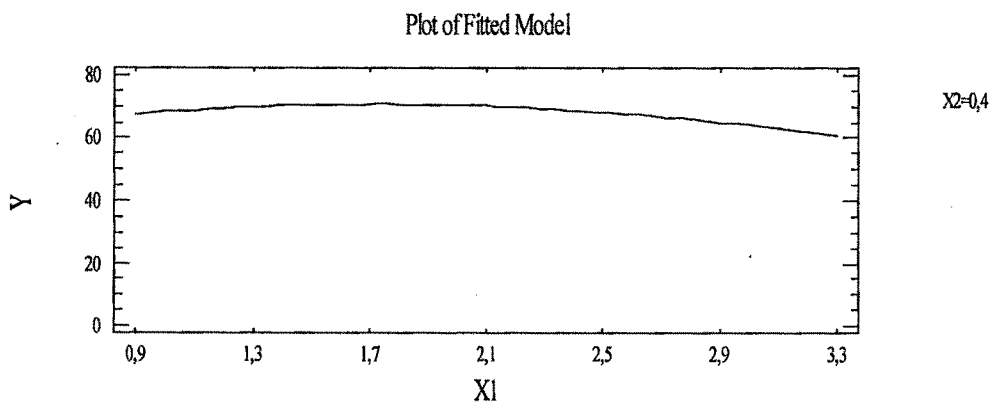

Figure 4.5.6 : Removal efficiency (Y) versus gas concentration (X_1) for constant liquid concentration ($X_2 = 0.4$) for nozzle N5

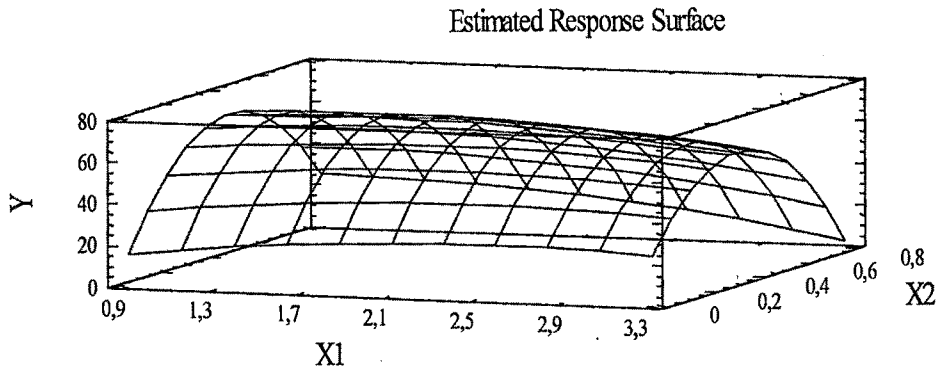

Figure 4.5.7: Removal efficiency (Y) response surface versus gas concentration (X_1) and liquid concentration (X_2) for nozzle N5

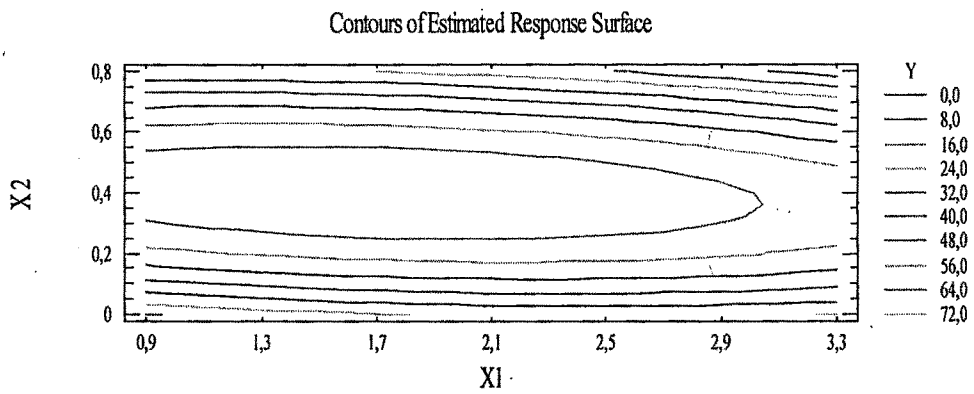

Figure 4.5.8 :Contour plot for removal efficiency (Y) for nozzle N5

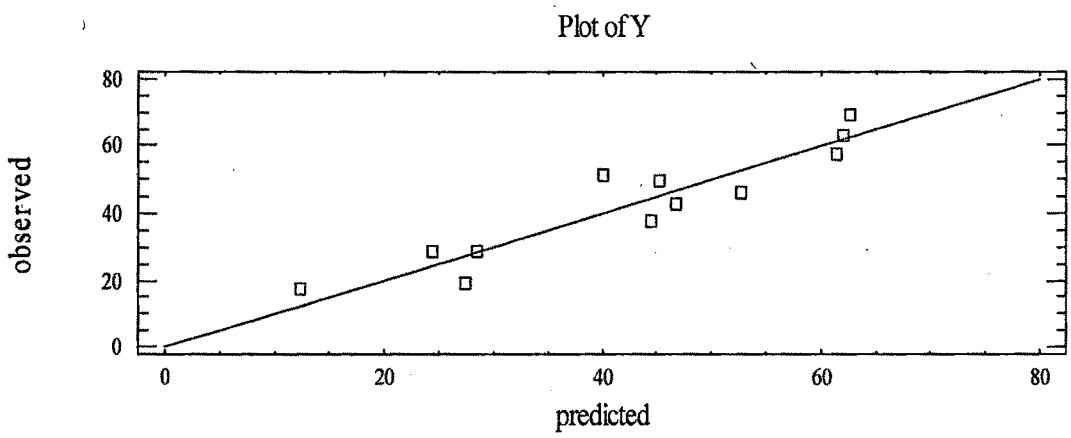

Figure 4.5.9 : Predicted removal efficiency (Y) versus observed removal efficiency (Y) for nozzle N5 for setup – 3 with no. of nozzle – 1

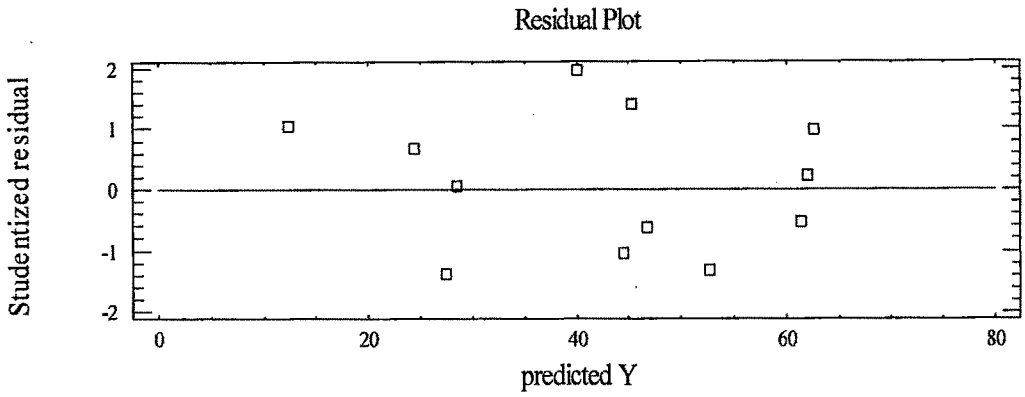

Figure 4.5.10 : Residual plot for nozzle N5

Nozzle N6 for Setup – 3 with no. of orifice 3

Table 4.5.C-1 : Estimation Results for nozzle N6

Parameter	Estimate	Asymptotic Standard Error	Asymptotic 95.0% Confidence Interval	
b1	67.9698	7.85634	48.746	87.1937
b2	-99.2834	42.5687	-203.445	4.87873
b11	-15.4581	2.76621	-22.2268	-8.6894
b22	95.9406	44.9216	-13.9789	205.86
b12	-17.0609	10.17	-41.9459	7.82414

Table 4.5.C-2 : Analysis of Variance for nozzle N6

Source	Sum of Squares	Df	Mean Square
Model	14787.6	5	2957.52
Residual	301.333	6	50.2222
Total	15088.9	11	
Total (Corr.)	2570.73	10	

Table 4.5.C-3 : Results of statistical tests for nozzle N6

R-Squared	88.2783 %
R-Squared (adjusted for d.f.)	80.4638 %
Standard Error of Est.	7.08676
Mean absolute error	4.43336
Durbin-Watson statistic	2.20699

Table 4.5.C-4 : Residual Analysis for nozzle N6

Estimation	Validation
N	11
MSE	50.2222
MAE	4.43336
MAPE	17.9304
ME	0.347291
MPE	-0.243646

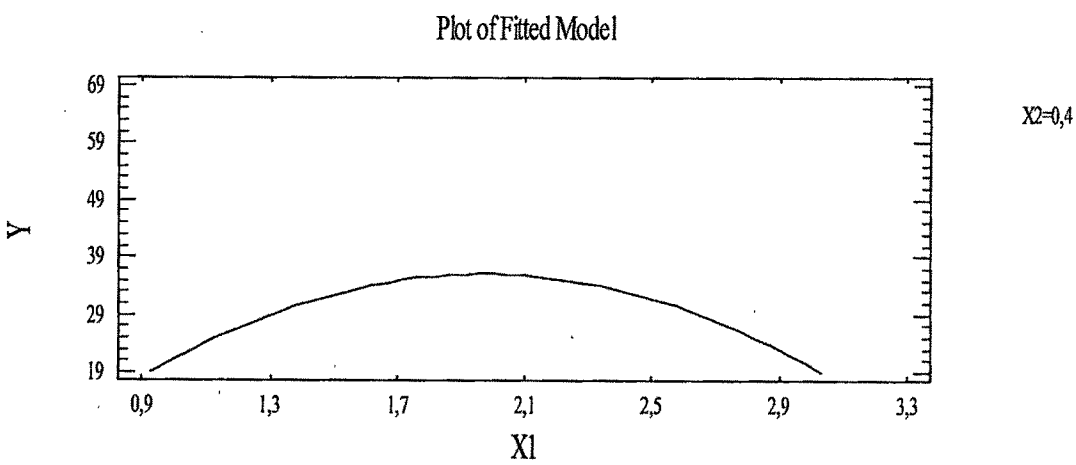

.Figure 4.5.11: Removal efficiency (Y) versus gas concentration (X_1) for constant liquid concentration (X_2 = 0.4) for nozzle N6

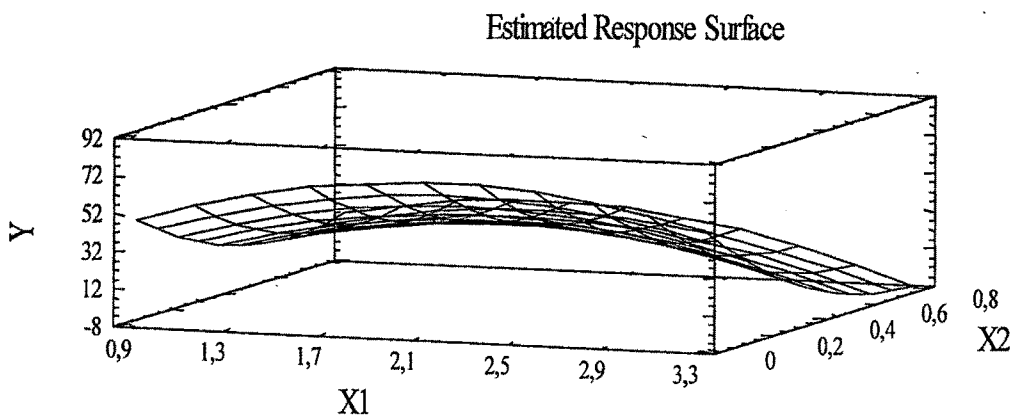

Figure 4.5.12 : Removal efficiency (Y) response surface versus gas concentration (X_1) and liquid concentration (X_2) for nozzle N6

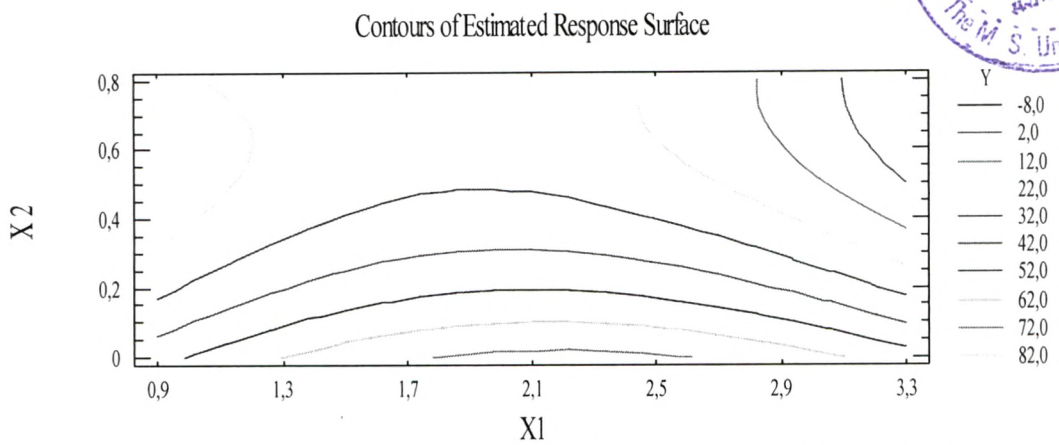

Figure 4.5.13: Contour plot for removal efficiency (Y) for nozzle N6

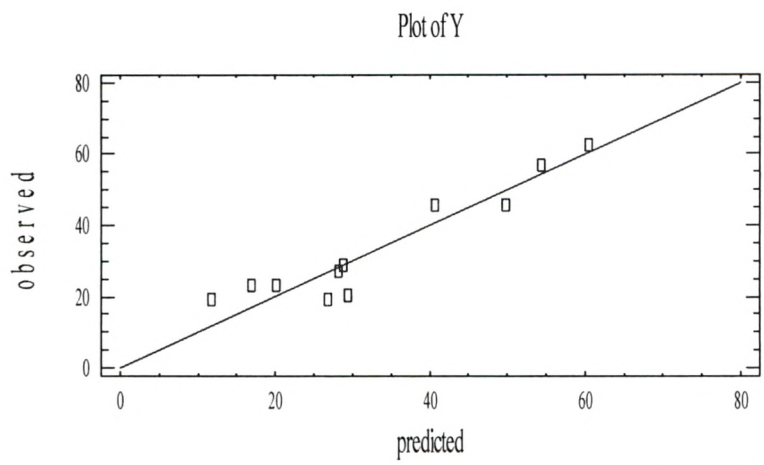

Figure 4.5.14 : Predicted removal efficiency (Y) versus observed removal efficiency (Y) for nozzle N6

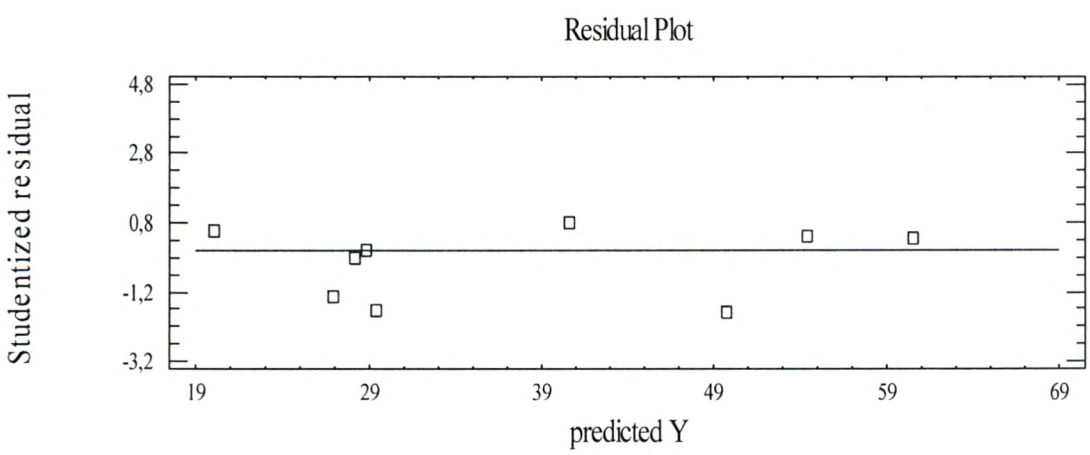

Figure 4.5.15 :Residual plot for nozzle N6

Nozzle N7 for Setup – 3 with no. of orifice 5

Table 4.5.D-1 : Estimation Results for nozzle N7

Parameter	Estimate	Asymptotic Standard Error	Confidence Interval Asymptotic 95.0%	
b1	17.4129	17.0439	-20.5635	55.3892
b2	166.782	82.0164	-15.962	349.527
b11	-0.923805	3.77345	-9.33159	7.48398
b22	-88.6827	92.8142	-295.486	118.121
b12	-19.0502	14.3113	-50.9379	12.8375

Table 4.5.D-2 : Analysis of Variance for nozzle N7

Source	Sum of Squares	Df	Mean Square
Model	64257.3	5	12851.5
Residual	10632.7	10	1063.27
Total	74890.1	15	
Total (Corr.)	7155.6	14	

Table 4.5.D-3 : Results of statistical tests for nozzle N7

R-Squared	-48.5931 %
R-Squared (adjusted for d.f.)	0.0 %
Standard Error of Est.	32.6079
Mean absolute error	17.9461
Durbin-Watson statistic	1.67242

Table 4.5.D-4 : Residual Analysis for nozzle N7

Estimation	Validation
n	15
MSE	1063.27
MAE	17.9461
MAPE	43.8221
ME	4.7561
MPE	-14.4586

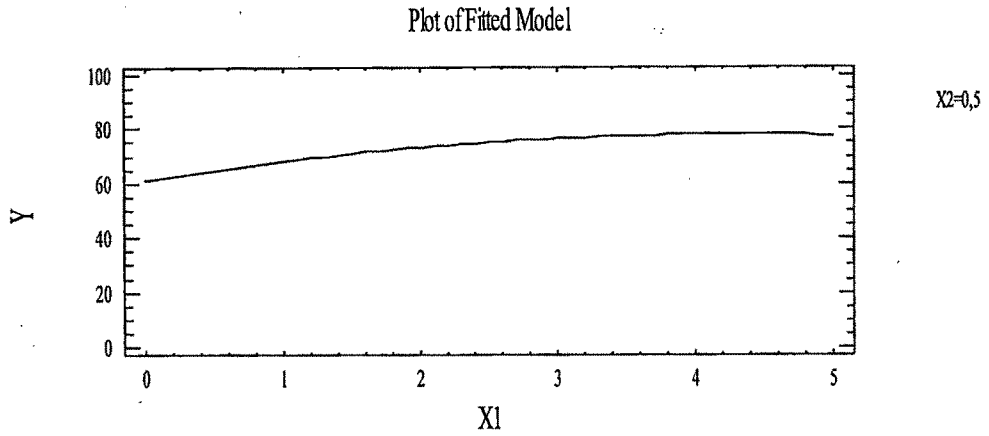

Figure 4.5.16:Removal efficiency (Y) versus gas concentration (X_1) for constant liquid concentration (X_2 = 0.5) for nozzle N7

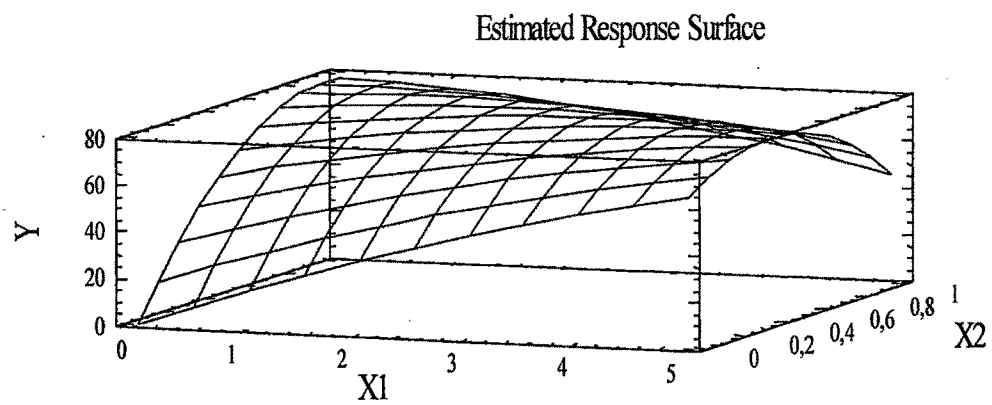

Figure 4.5.17: Removal efficiency (Y) response surface versus gas concentration (X_1) and liquid concentration (X_2) for nozzle N7

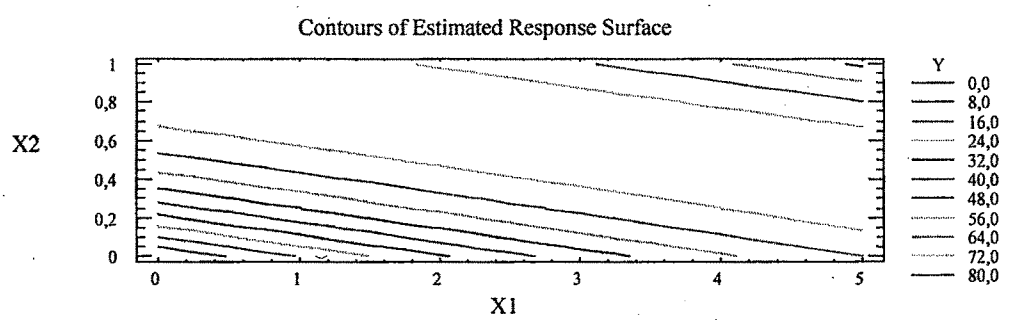

Figure 4.5.18:Contour plot for removal efficiency (Y) for nozzle N7

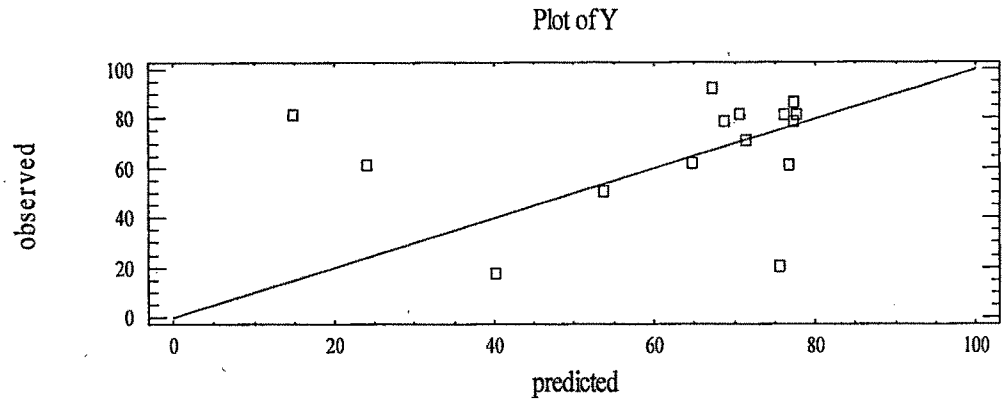

Figure 4.5.19 : Predicted removal efficiency (Y) versus observed removal efficiency (Y) for nozzle N7

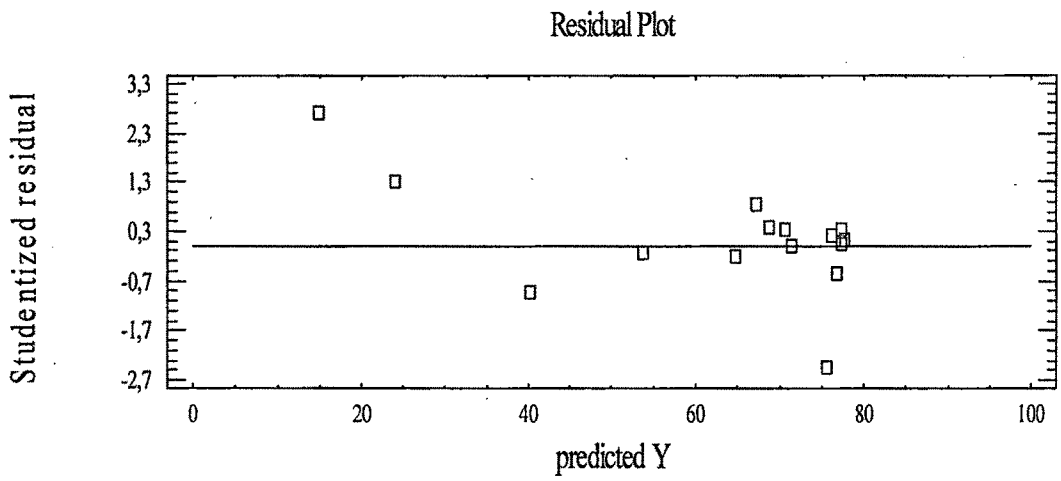

Figure 4.5.20 : Residual plot for nozzle N7

4.5.2.3 Interpretation of the results of statistical analysis in STATGRAPHICS Plus 4 for different nozzles

The results of fitted model, R-squared test, R-squared (adjusted for d.f.) test, standard error of estimates, mean absolute error and Durbin-Watson statistic test are summarized in table (4.5.6) and may be interpreted as follow.

- The R-Squared statistic indicates that the model as fitted explains 85.84% , 86.55 %, 88.27% and 48.59% of the variability in Y for N1, N5, N6 and N7 respectively.

- The adjusted R-Squared statistic which is more suitable for comparing models with different numbers of independent variables are 77.75%,78.86%, 80.46% and 0.0% for N1, N5, N6 and N7 respectively
- The standard error of the estimate shows the standard deviation of the residuals to be 9.79, 7.69, 7.08 and 32.60 for N1, N5, N6 and N7 respectively. This value can be used to construct prediction limits for new observations.
- The mean absolute error (MAE) of 6.18, 5.15, 4.43 and 17.94 is the average value of the residuals for N1, N5, N6 and N7 respectively

Table 4.5.6 : Summary of statically results

Set Up	Fitted Model	R-Squared	R-Squared (adjusted for d.f.)	Standard Error of Est.	Mean absolute error	Durbin-Watson statistic
N1	$Y = 11.1059X_1 + 205.385X_2 + 0.688086X_1X_1 \pm 72.5912X_2X_2 \pm 56.7127X_1X_2$	85.8423%	77.7522%.	9.79912	6.18318	0.891519
N5	$Y = 20.6505X_1 + 263.417X_2 - 4.09009X_1X_1 \pm 293.901X_2X_2 \pm 16.134X_1X_2$	86.5528 %	78.8687 %	7.69463	5.15937	1.95717
N6	$Y = 67.9698X_1 - 99.2834X_2 - 15.4581X_1X_1 + 95.9406X_2X_2 \pm 17.0609X_1X_2$	88.2783%	80.4638%	7.08676	4.43336	2.20699
N7	$Y = 17.4129X_1 + 166.782X_2 - 0.923805X_1X_1 \pm 88.6827X_2X_2 \pm 19.0502X_1X_2$	48.5931%	0.0 %	32.6079	17.9461	1.67242

- The Durbin-Watson (DW) statistic tests the residuals to determine if there is any significant correlation based on the order in which they occur. Since, the DW value is less than 1.4 for N1 there may be some indication of serial correlation. Similarly, since, the DW value is greater than 1.4 for N5, N6, N7 there is probably not any serious autocorrelation in the residuals.
- The output also shows asymptotic 95.0% confidence intervals for each of the unknown parameters.

4.5.2.4 Interpretation of figures (graphs)

For each set of experiment a mathematical model describing the effect of related variables on removal efficiency were derived and plotted in the figures (4.5.1) to (4.5.20).These figures may be analyzed as follows:

Figures (4.5.2), (4.5.7), (4.5.12) and (4.5.17) show the response surfaces for the removal of chlorine with variation in initial gas concentration and the scrubbing liquid concentration. The response surface shows removal efficiency varies from 50% to maximum value of 95%. It is observed that the effect of liquid concentration is greater than the gas concentration on RE.

Dependency of removal efficiency (RE) on gas concentration ($C_{Ag,in}$) and on initial concentration of liquid (C_{B0})

Figures (4.5.1), (4.5.6), (4.5.11) and (4.5.16) are demonstrative curve of the fitted model showing the effect of $C_{Ag,in}$ on $\%RE$ at constant C_{B0}.The similar curve may be obtained and plotted for other value of C_{B0}.

Figures (4.5.3), (4.5.8), (4.5.13) and (4.5.18) show the contours of estimated response surface for nozzle N5, N6, N7 and N1 respectively. The presentation of contours is for visualization of the best region where the $\%RE$ is maximum.

A common trend (except small variation for nozzle N6) may be observed that at higher concentration of C_{B0} there is decrease of $\%RE$ with increase in initial concentration of $C_{Ag,in}$. But a reverse trend is observed at lower C_{B0} i.e. $\%RE$ is increasing with increase in $C_{Ag,in}$. The reason for this behavior is that at higher C_{B0} the viscosity of liquid increases. The higher

viscosity has adverse effect on diffusivity and physical solubility. And this effect becomes more appreciable at higher $C_{Ag,in}$ because of higher scrubbing load due to higher initial concentration of A ($C_{Ag,in} - C_{Ag,out}$).

The figures (4.5.3), (4.5.8), (4.5.13) and (4.5.18) showing contours have significance that they show the correlations of all the parameters .The counters are useful to identify the regions of maximum efficiency The following table shows the regions of the maximum efficiency.

Analysis of the contours suggests the following regions to have maximum RE.

Table 4.5.7 : Summary of analysis of contours for removal efficiency

Nozzle No.	Best region $C_{Ag,in}$	Best region C_{B0}	Maximum efficiency achievable
N1	$(0.9 - 2.4) \times 10^{-3}$	1.5- 0	90
N5	0.9 – 3.3 0.9 – 3.3	0.02 -0 0.8 – 0.75	72
N6	0.9 – 1.2 2.5 – 3.3	0.3 – 0.8 0.8 – 0.25	82
N7	0 – 2.00	0.2 – 0	80

Observed versus Predicted $\%RE$

The figures (4.5.4), (4.5.9), (4.5.14) and (4.5.19) show the observed versus predicted plot for N1, N5, N6 and N7 respectively. The Y axis shows the observed value of $\%RE$ and X axis show the predicted value by fitted model of $\%RE$. It may be observed that the points are randomly scattered around the diagonal line indicating that model fits well. It may also be observed that the plot is straight line having no curve that means no need to try for higher order polynomial.

Residuals versus Predicted

The figures (4.5.5), (4.5.10), (4.5.15) and (4.5.20) show of the residual analysis. The Y axis shows Studentized residual and X axis shows the predicted $\%RE$ from the fitted models. It may be observed that there is uniformity in variability with change in mean value shown by line in the center.

4.5.3 Conclusion

The models developed as shown in table (4.5.4) for nozzles N1, N5, N6 and N7 to predict $\%RE$ by using STATGRAPHICS considering variation with respect to $C_{Ag,in}$ and C_{B0} are well fitted.

Statistical analysis showed that both factors C_{B0} and $C_{Ag,in}$ have significant effect on removal efficiency (RE) but the liquid concentration is more significant between two.